Review

Not peer-reviewed version

Metal Organic Framework (MOF): Synthesis and Fabrication for the Application of Electrochemical Sensing

Ricky Lalawmpuia , Melody Lalhruaitluangi , Lalhmunsiama Lalhmunsiama , Diwakar Tiwari * , Jae-Kyu Yang *

Posted Date: 4 September 2023

doi: 10.20944/preprints202309.0192.v1

Keywords: advanced materials; metal organic framework; electrochemical sensor; trace detection; emerging pollutants

Review

Metal Organic Framework (MOF): Synthesis and Fabrication for the Application of Electrochemical Sensing

Ricky Lalawmpuia [1], Melody Lalhruaitluangi [1], Lalhmunsiama [2], Diwakar Tiwari [1,*] and Jae-Kyu Yang [3,*]

[1] Department of Chemistry, School of Physical Sciences, Mizoram University, Aizawl-796004, India
[2] Department of Industrial Chemistry, School of Physical Sciences, Mizoram University, Aizawl-796004, India
[3] Department of Environmental Engineering, Kwangwoon University, Seoul 01897, Republic of Korea
* Correspondence: jkyang@kw.ac.kr (J.-K.Y.); diw_tiwari@yahoo.com (D.T.); Tel.: +82-02-940-5769 (J.-K.Y.); +91-9862323015 (D.T.); https://orcid.org/0000-0003-3784-9422 (J.-K.Y.); https://orcid.org/0000-0002-9177-9704 (D.T.)

Abstract: Metal-organic framework (MOF) is a porous hybrid material of metal ions connected by organic bridging ligands. The coordination bonds link the metal ions, metal-ion clusters, and organic ligands to create the MOFs, and the materials are a distinctive class of crystalline frameworks. These porous materials possess relatively large surface area, tunable pore sizes, various functionalities, and high thermal stability. Therefore, diverse area of research including electrochemical sensor development utilizes distinctive and engineered MOFs materials. The review critically analyzes the strategy adopted for synthesizing a variety of MOFs materials. The role of these engineered materials in the fabrication of a miniaturized device demonstrates the detection of various emerging water contaminants in an aqueous medium. The studies demonstrated an understanding of the insights of sensor and device development. Moreover, the challenges encountered utilizing the MOFs in the electrochemical sensor development are precisely included, along with future perspectives of these studies.

Keywords: advanced materials; metal organic framework; electrochemical sensor; trace detection; emerging pollutants

1. Introduction

Metal-organic framework (MOF) is a category of porous materials that have drawn greater attention a few decades back. The MOF are primarily hybrid materials having organic and inorganic moieties. The organic linker in its structure comprises organic ligands, with the metal cluster acting as inorganic components [1]. The target MOF is distinguished or embedded by the functional groups among metal nodes and organic linkers, supporting the selectivity and reliability of materials for specific purposes, including electrochemical sensing [2]. The MOF showed varied applications in the area of gas adsorption [3], catalysis [4], optical storage media [5], drug delivery [6], sensing, separation [7], redox-active electrode materials [8], etc. due to its micro-to-meso porous structure, high surface area, and flexible structures. Increasing the electrocatalytic signal by immobilizing the metal nanoparticles within the pores of MOFs is advantageous, resulting in suitable and sensitive sensing [9].

The MOFs showed numerous advantages over conventional porous materials due to the high surface area, pore working capabilities, and regulated shape and size of pores due to using suitable organic linkers in the material synthesis [9]. Due to their distinctive properties, MOFs are known hybrid materials with possible applicability in electrochemical sensing techniques for determining or detecting various micro-pollutants and heavy metals in aquatic environments [10]. Initially, the

MOFs were derived using the divalent cations of transition metals *viz*, zinc (Zn^{2+}), cobalt (Co^{2+}), copper (Cu^{2+}), etc. including well known MOFs such as MOF-5, HKUST-1, ZIF-8 etc. The use of divalent transition ions makes easy crystallization of synthesized MOF; however, divalent cations showed several disadvantages, such as low hydrothermal stability that impacts the annealing of materials and even some of the applications [11]. Therefore, the selection of metal cations in the synthesis of MOF is crucial. Further, the thermodynamic studies indicated that higher-charged metal cations possess strong metal-ligand bonds, significantly enhancing MOF's hydrothermal stability [12]. The stability of the MOF increases with higher valency ions such as iron (Fe), aluminum (Al), zirconium (Zr), and titanium (Ti), which indicated that metal ions with greater valency are more stable than those of divalent metal cations such as zinc (Zn), copper (Cu) and cobalt (Co). In addition, aluminum is abundant on the Earth's crust, cheap, and lightweight, enabling large-scale production of MOF for varied applications such as removing pollutants, sensors, and storing gases [13].

Voltammetry and amperometry are the most reliable and efficient electroanalytical techniques for the qualitative and quantitative determination of several analytes at trace levels due to their reasonably high sensitivity, robust instrumentation, and relatively cost-effective compared to other spectroscopic or chromatographic techniques. The core component of the electroanalytical techniques is the working electrode at which the analytes react electrochemically. The electrodes fabricated with suitable materials have ability a selective oxidation or reduction of analyte [14]. Many typical electrodes have poor surface kinetics, significantly decrease selectivity and sensitivity. This is known to cause a variety of key difficulties. Analytes often exhibit a broad peak on standard electrodes, with no peak seen at lower concentrations [15].

Similarly, the MOFs have a practical choice because of their ability to selectively analyze the analytes of interest, enabling them to detect them efficiently. The application of MOFs in electroanalytical methods is a relatively newer approach, and several challenges have been found in designing an attractive and intriguing framework for detecting the target analytes or biomolecules in aqueous media [16]. The MOFs are the designed materials, and properties alter as per the specific applications; hence, the MOFs are the futuristic engineered materials with varied applications in diverse research areas. Furthermore, MOFs, in general, possess unique properties such as high specific surface area, pore volume, molecular sizes of the pores, and flexibility of the framework that is responsive (adaptive) towards the target adsorbate ions/molecules. The application of MOFs in modifying carbon-based electrode studies for sensing and detecting several analytes in the literature. However, designing and fabricating the miniaturized device development utilizing the engineered metal-organic frameworks is the futuristic application of MOFs. The main goal of this review is to highlight the synthesis of various kinds of MOFs and focus on the application of the synthesized MOFs in sensing using electroanalytical techniques to detect potential water contaminants at trace levels.

2. Synthesis of MOF

Metal-organic frameworks (MOFs), built from inorganic nodes and organic linkers, have drawn much interest because of their structural variety, rarity of properties, and capacity to customize for specific functions. The organic linkers and metal centers design the structure of MOFs appropriately; the organic linkers participate in shear connections, and the metal centers act as joints [17]. There are several methods to synthesize the MOFs, which are briefly discuss below.

2.1. Hydrothermal/Solvothermal Synthesis

Hydrothermal synthesis is typically adopted to produce sustainable metal-ligand bonds across the framework, which yields the most comprehensive dynamical products [18]. Long-term heating of the reaction mixture at high pressures and temperatures requires hydrothermal synthesis of MOF [19]. Based on the material's dissolution rate in hot water under intense vapor pressure upheld at a temperature variation between the reactor's opposite nodes yields single crystals. Moreover, the 'solvothermal' process utilizes suitable solvents besides water in the material synthesis. The method results from the growth of high-quality crystals and is appropriate for materials with vapor pressure

Preprints (www.preprints.org) | NOT PEER-REVIEWED | Posted: 4 September 2023 doi:10.20944/preprints202309.0192.v1

close to their melting points [20]. Figure 1 illustrates a schematic of the steps in the synthetic approach using hydrothermal and solvothermal processes.

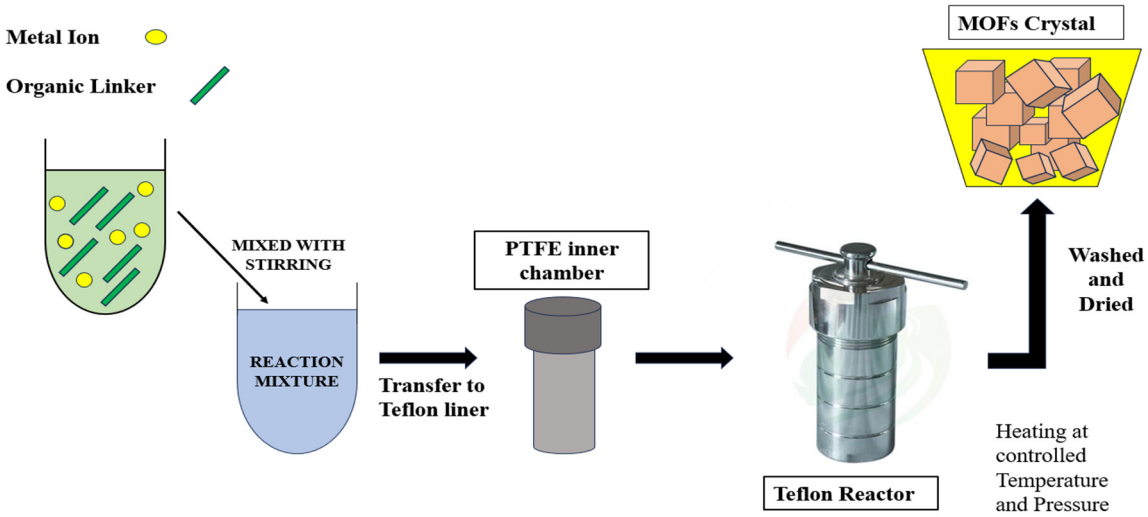

Figure 1. Schematic of the hydrothermal/solvothermal synthesis of metal organic frameworks.

The hydrothermal method synthesizes the Cu (4, 4′-bpy)$NO_3(H_2O)$ crystals with rectangular parallelepiped-shaped, utilizing the 4, 4′-bipyridine as a nitrogen donor aromatic ligand [21]. Similarly, the hydrothermal method synthesizes the Cu (copper) benzene-1, 3, 5-tricarboxylate (TMA) $[Cu_3(TMA)_2(H_2O)_3]_n$ complex known as HKUST-1 using the carboxylic as functional group [11]. Transition metals (cobalt, nickel, and zinc) based MOFs were obtained using the hydrothermal route by simple metal ions self-assembling at the adaptive bis-(imidazole) binding sites [22]. The hydrothermal reaction yielded a polycrystalline Fe-MIL-100 powder with a significantly large attainable and enduring porosity, demonstrating an intriguing Friedel-Crafts reaction with catalytic activity employing the redox properties of Fe(III) [23]. Ni(II) is a typical transition metal ion with varied interest because of its inexpensive cost, high abundance, superior catalytic activity, and electrochemical characteristics [24,25]. Ni-MOFs are synthesized by the hydrothermal process using Ni(II) and the 1,3,5-benzene tricarboxylate as a ligand [26]. Nickel-based compounds with the proper design showed considerable potential for usage in the electrochemical industry as electrode surface modifications and electrocatalysts [27–29].

2.2. Ultrasonic methods

The ultrasonic-assisted synthesis offers relatively environment-friendly conditions for MOFs synthesis in ambient reaction conditions (i.e., ambient temperature and atmospheric pressure) with less reaction time. Furthermore, the ultrasonic-assisted synthesis approaches avoid safety concerns, providing an opportunity to expand on the twelve principles of green chemistry [30]. Among several MOF synthetic techniques, the ultrasonication method is affordable and environmentally benign. It could produce a high yield while operating under ambient temperature and pressure in a solvent-free reaction [31].

Compared to other methods, ultrasonic-aided MOF synthesis is practically viable, containable, and quickly produces the product with a significant yield [32]. Ultrasonic cavitation for producing MOFs is relatively new and has recently attracted greater attention [33]. In 2009, Khan et al. [34] conducted the first study on the impact of ultrasonic irradiation on the Cu-BTC MOF. The ultrasonically assisted synthesis of MOFs significantly reduces the reaction time compared to the electronically controlled and microwave heating methods. Additionally, a limited sonication enabled the shrinking of size of the MOF particles; however, an increased sonication time from 6 to 45 min caused aggregation of the MOFs [35].

Preprints (www.preprints.org) | NOT PEER-REVIEWED | Posted: 4 September 2023 doi:10.20944/preprints202309.0192.v1

On the other hand, Taghipour et al. reported the possible role of solvent in the yield of MOF production using the ultrasound method [36]. The effect of the solvents (binary and ternary mixtures) on the textural properties of Cu-BTC investigates the ultrasonic parameters, such as sonication duration and power, thoroughly explored in the synthesis of MOFs (Figure 2). A ternary mixture of solvents viz., water, ethanol, and N-dimethylformamide (DMF) sonicated for 120 min at a power of 750 W resulted in an enhanced yield of Cu-MOF [36].

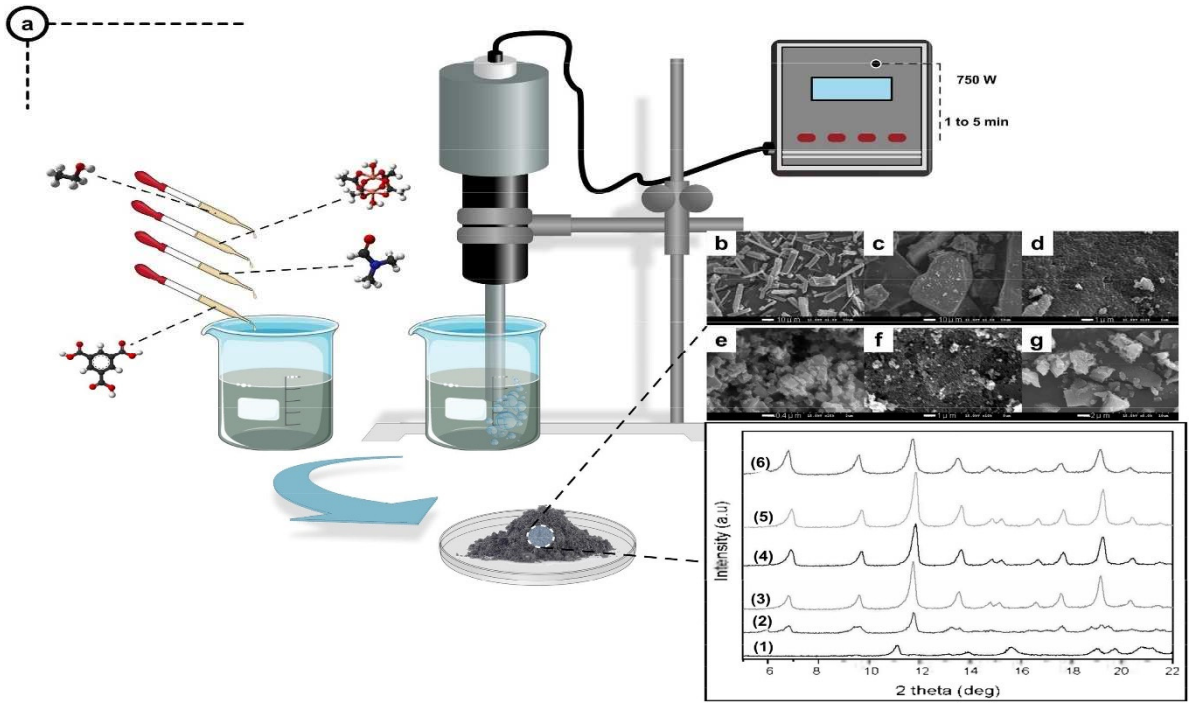

Figure 2. Schematic of Cu-BTC production with ultrasonic assistance and SEM images of MOF with varying DMF concentrations during sonication for 1 min [36].

2.3. Microwave-aided synthesis

Microwave-aided synthesis is the most efficient approach for carrying out many reactions. Compared to conventional solvothermal synthesis, microwave irradiation reduces the reaction time and enhances the crystal growth of porous materials that take several days or weeks in conventional methods [37]. The microwave irradiation energy, time of exposure, solvent concentration, and solvent systems are the key parameters regulating the yield and crystal growth of the MOFs, and microwave irradiation showed a positive impact on material characteristics and properties [38]. Microwave-assisted synthesis acknowledges rapid heating, fast kinetics, phase purity, increased yield, improved dependability, and repeatability over hydrothermal synthesis [39–42]. Additionally, it offers an effective method to regulate the distribution of macroscopic morphology, particle size, and phase selectivity during the synthesis of inorganic solids and nanocomposite materials. Although the synthesis is substantially faster, the characteristics of the crystals produced by the microwave-assisted approach are on par with those produced by the conventional solvothermal process [43–45]. However, microwave-assisted methods have received greater interest investigating the effect of irradiation period, power, temperature, solvent concentration, and metal ion/organic linker ratio, for example, on the synthesis of MOF-5 by employing the microwave-assisted technique [46]. The nanocrystal crystallization process optimizes for several parameters: time, temperature, and power such as 1 h at 130 °C and 600-1000 W, respectively. This study showed that the crystal formation occurred under microwave irradiation of 15 min and produced a high-quality crystal between 30 min and 24 h. Similarly, microwave-assisted synthesis produces the Zr-based MOF (Zr-fum-fcu-MOF)

Preprints (www.preprints.org) | NOT PEER-REVIEWED | Posted: 4 September 2023 doi:10.20944/preprints202309.0192.v1

having the octahedral shape at the reaction temperature of 100 °C. The schematic of the synthesis process is shown in Figure 3 [47].

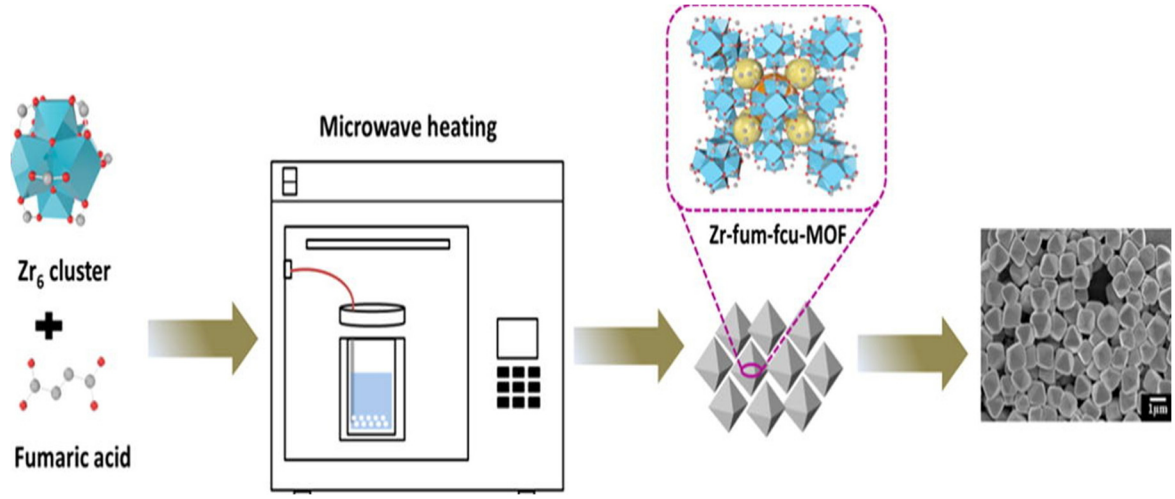

Figure 3. Microwave assisted synthesis of Zr (fumarate-face centered cubic) MOF [47].

2.4. Electrochemical synthesis

The electrochemical process of MOF synthesis possesses several advantages over conventional MOF synthesis, including relatively short reaction time, relatively simple equipment setup, real-time MOF structure modification, quick synthesis, no need for precursor metal salts, and direct accumulation of MOFs on the preferred substrates, etc. [48,49]. In addition to its simple process, the electrochemical synthesis of MOFs has provided numerous favorable circumstances, such as random and quick synthesis with lesser use of linker and solvent, excellent yield, and low energy consumption [50]. The mild reaction conditions, which perform at ambient temperature and pressure, are the most attractive feature of electrochemical synthesis. Despite these advantages, it remains a less utilized approach, particularly in synthesizing functionalized framework materials [51]. This approach also constantly altered the real-time response, enabling the direct output of crack-free nanostructures in the absence of a pre-treated surface at high temperatures.

On the other hand, relatively high reaction temperatures, longer reaction times, and thermal-induced cracking on the films are shown in the solvothermal or hydrothermal techniques [52]. Zn-based MOF was synthesized electrochemically using the electrochemical method, and the physicochemical parameters, viz., reaction time, electrolyte quantity, current, and voltage, are optimized for greater yield of the solid. The results indicated that both reaction time and current density significantly impacted the purity and yield, and it was observed that an applied current of 60 mA and a reaction time of 2 h yielded 87% of the product [53]. Figure 4 shows the instrumentation of a simple electrochemical synthesis of $Zn_3(BTC)_2$-MOF [54].

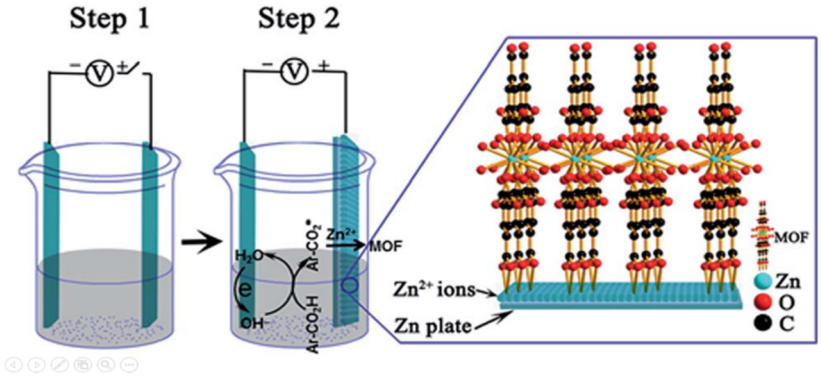

Figure 4. Electrochemical synthesis of $Zn_3(BTC)_2$-MOF [54].

Preprints (www.preprints.org) | NOT PEER-REVIEWED | Posted: 4 September 2023 doi:10.20944/preprints202309.0192.v1

2.5. Mechanochemical synthesis

Mechanochemical synthesis is one of the most exciting chemical modifications employed to obtain high purity with enhanced yield of several MOFs [55]. Most coordination polymerization processes involving multisite ligands with metal ions proceed readily in a suitable solution environment. The solvent-free or solid-state formation of MOFs without any toxic or hazardous solvents has progressively received attention in recent years due to significant advances in mechanochemical synthesis [50]. Coordination polymerization, broadly, involves the reaction in the presence of solution, multisite ligands, and metal ions. Nonetheless, the mechanochemical synthesis of MOFs is less solvent-intensive, solvent-free, or a solid-state organic process devoid of unpleasant and harmful solvents [56].

Furthermore, compared to the diffusion and solvothermal methods, this technique is advantageous for large-scale MOF manufacturing in a shorter reaction time and at room temperature [57,58]. The solid-solid reaction has the potential to synthesize a large-scale production of materials and provides simplicity in handling since it directly produces the products in powdered forms. Although mechanochemical synthesis is a "solvent-free" or "solvent-less" process, a solvent-based purification step is still required. Despite this, the mechanochemical synthesis is reasonably environment friendly and is anticipated to be commercially exciting for MOFs production [59]. The liquid-assisted mechanochemical synthesis produced the MOF-5, showing that the solid possessed a relatively low BET area and contained many amide precursor by-products [60]. A copper-based MOF with a product yield of 97% was synthesized in the mechanochemical process using the $Cu(OAc)_2.H_2O$ and H_3btc. A dark blue color solid was obtained at 30 Hz and 20 min of reaction time [55]. The framework structures produced by the mechanochemical method are easily separable from the host molecules, providing repeatable free pore access for additional uses [61]. The synthesis of HKUST-1 and MOF-14 showed the method's applicability in efficient MOFs production [55]. Figure 5 demonstrates the mechanochemical method of synthesizing MOF.

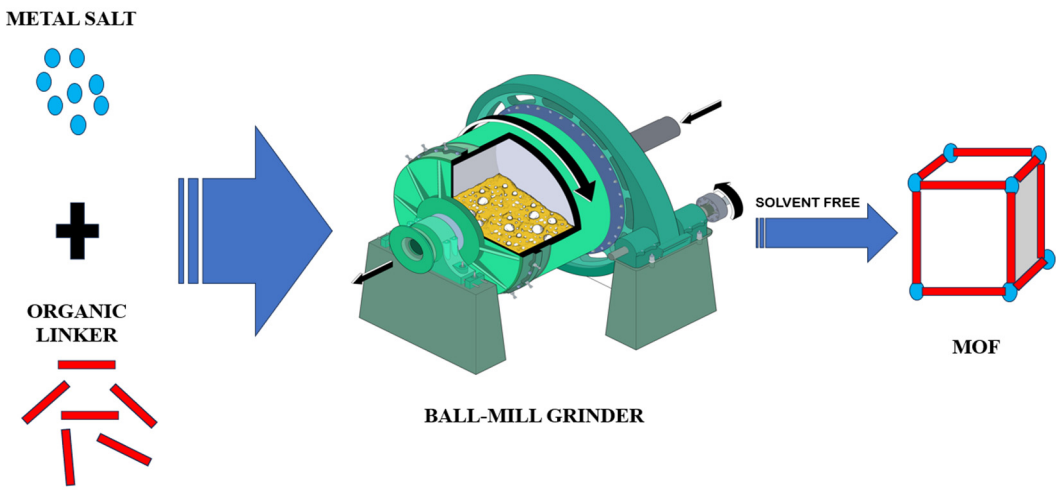

Figure 5. Schematic of mechanochemical synthesis of MOF.

The different types of MOF have different routes of synthesis. The organic linker should be chosen wisely depending on the central metal atom. Table 1 displays the different types of MOF synthesized using different routes under varying conditions.

Preprints (www.preprints.org) | NOT PEER-REVIEWED | Posted: 4 September 2023 doi:10.20944/preprints202309.0192.v1

Table 1. Synthesis of different MOFs obtained by different methods.

	Sample	Metal	Ligand	Solvent	Condition	Ref.
Hydrothermal synthesis	UiO-66	$ZrCl_4$	H_2BDC	DMF	120℃, 24 h	[62]
	Co-MOF	$Co(NO_3)_2{\cdot}6H_2O$	H_3BTC	DMF	100℃, 24 h	[63]
	Ni-MOF	$Ni(NO_3)_2{\cdot}6H_2O$	H_3BTC	DMF	80℃, 18 h	[64]
	MIL-53	$FeCl_3{\cdot}6H_2O$	H_2BDC	DMF	150℃, 15 h	[65]
	Ce-MOF	$Ce(NO_3)_3{\cdot}6H_2O$	H_3BTC	DMF-Ethanol	120℃, 2 h	[66]
	Cu-NH_2BDC	$Cu(NO_3)_2{\cdot}3H_2O$	NH_2BDC	DMF-Ethanol	110℃, 20 h	[67]
	MIL-101	$Cr(NO_3)_3{\cdot}9H_2O$	H_2BDC	De-ionized water	180℃, 5 h	[68]
Ultrasound	MOF-5	$Zn(NO_3)_2{\cdot}6H_2O$	H_2BDC	DMF	90 W, 2 min	[69]
	ZIF-8	$Zn(NO_3)_2{\cdot}6H_2O$	MeIM	DMF	300 W, 1 h	[70]
	MOF-74	$Mg(NO_3)_2{\cdot}6H_2O$	H_4dhtp	DMF	500 W, 1 h	[71]
	Sn-BDC	$SnSO_4$	Na_2BDC	De-ionized water	155 W, 5 min	[72]
	HKUST-1	Copper(II) nitrate hemipentahydrate	H_3BTC	DMF	130 W, 1 h	[73]
Microwave method	Ni-MOF-74	$Ni(NO_3)_2{\cdot}6H_2O$	DOT	DMF	100℃, 90 min	[74]
	Mg-MOF	$Mg(NO_3)_2{\cdot}6H_2O$	DOT	DMF	125℃, 90 min	[74]
	MOF-5	$Zn(NO_3)_2{\cdot}6H_2O$	H_2BDC	DMF	300 W, 2.5 min	[75]
	MOF-177	$Zn(NO_3)_2{\cdot}6H_2O$	H_3BTB	NMP	800 W, 35 min	[76]
	MOF-199	$Cu(NO_3)_2{\cdot}3H_2O$	H_3BTC	DMF	250 W, 30 min	[77]
Electrochemical synthesis	Co-MOF	$Co(NO_3)_2{\cdot}6H_2O$	H_3BTC	H_2O, ethanol	Electrolyte (Et_3NHCl)·$6H_2O$	[78]
	HKUST-1	Cu foil electrode	H_3BTC	DMSO, ethanol	Electrolyte (MTBAMS)	[79]
	HKUST-1	Cu electrode	H_3BTC	Methanol	Electrolyte (TBATFB)	[80]
	Cu-MOF	$Cu(NO_3)_2{\cdot}3H_2O$	H_4BTEC	DMF, H_2O	Electrolyte (TBATFB)	[81]
Mechanochemical synthesis	Cu-MOF	$Cu(OAc)_2{\cdot}H_2O$	H_3BTC	No solvent	15.0 min	[82]
	MIL-88A	$FeCl_3{\cdot}6H_2O$	Furmarate	No solvent	10.0 min	[83]
	MOF-505	$Cu(OAc)_2{\cdot}H_2O$	H_4bptc	DMF	40.0 Hz, 80 min	[84]
	IRMOF-3	$Zn_4(\mu_4O)(NHOCPh)_6$	NH_2BDC	No solvent	30.0 Hz, 30 min	[85]

3. Design and fabrication of MOF-based sensors

Due to their high porosity, enormous surface area, and cavity structures, MOFs are valuable in electrochemical sensor applications. These unique properties provide MOFs with a high-level catalytic feature. Moreover, the robust use of these materials on the electrode surface enables efficient development of electrochemical sensors. The MOF materials' high porosity and surface area enhance these sensors' detection sensitivity [86]. MOFs show low electronic conduction properties due to their poor overlapping between the electronic states and frontier orbitals of ligand and metal ions [87,88]. Therefore, the direct use of pure MOFs on electrodes or other electroanalytical methods is limited [89–91]. A recent report uses the carbon-based materials *viz.*, fullerenes (C60), graphene, and multi-wall carbon nanotubes (MWCNTs) for the modification of nickel-based MOF, which shows an increased electrical conductivity with decreased charge transfer resistance, high porosity, and large surface area. These composite materials showed enhanced applications in sensor developments [92].

3.1. Carbon based electrode modification by MOF

Among several electrode modifiers used in electrochemical processes, MOFs have shown potential due to their large surface area, copious adsorption sites, and versatile functionality that helps trace and efficiently detect several analytes, including heavy metal ions [93,94]. In general, the carbon allotropes deployed in the fabrication of electrodes are graphite or derived materials intended to modify the carbon paste electrode (CPE) and glassy carbon (GC) for solid carbon electrodes. The conductivity of carbon-based materials allotropes is enhanced primarily due to sp^2 hybridized bonds and six-membered aromatic rings [95]. It is essential to pre-modify carbon-based electrodes to follow a specific protocol for introducing MOF modifiers at the electrode surface. In the case of glassy carbon electrodes, the modification involves a direct coating of the polished surface by MOF. In contrast, the modifier was first synthesized in a carbon paste electrode by mixing graphite powder with MOF using a specific organic binder [96].

Preprints (www.preprints.org) | NOT PEER-REVIEWED | Posted: 4 September 2023 doi:10.20944/preprints202309.0192.v1

3.1.1. MOF modified carbon paste electrode (CPE)

One of the most often utilized electrodes recently is the carbon paste electrode because of its easy and versatile fabrication [97]. The carbon paste electrodes are inexpensive and made by blending graphite with MOF along with a suitable organic binder. High-purity graphite powder with a particle size of 1 to 10 micrometers fabricates electrodes [98]. Further, the purity of the graphite powder greatly influences the electrochemical performance of the electrodes [99]. In addition, the organic binder helps the modifier (MOF) bind at the electrode surface, which must be stable, insoluble, and impurities-free. Paraffin oils, aliphatic and aromatic hydrocarbons, silicone oils and greases, halogenated hydrocarbons, and similar derivatives are popularly used as CPE binders for CPEs [100]. Graphite powder has high electrical conductivity; hence, it is easy to fabricate the MOF-modified carbon paste electrodes in the electrochemical processes [101]. In typical CPEs, the modifier (MOF) acts as a Lewis acid in catalysis, which further helps decrease the sensor's overpotential and charge transfer resistance. Also, the distinct pore size elevates the selective determination of various analytes in the complex matrix [102].

Carbon paste electrodes are fabricated using graphite powder as a modifier and organic binder. The mixture is mixed in an agate mortar to obtain a well-distributed suspension placed into an electrode frame. The electrical connections often utilize the copper, titanium, or platinum wires. Teflon tube having a diameter of Ca. 0.5 cm is used as the electrode frame. The graphite powder and paraffin binder were mixed at 7:3 and then introduced into the electrode frame, and a copper wire was used as electrical contact [103]. The duplicating paper polishes the fabricated electrode surface.

Additionally, two approaches demonstrate the carbon paste electrode fabrication, viz., the *in-situ* and *ex-situ* approaches [104]. The *in-situ* fabrication utilizes the modifier (MOF) with graphite powder. The disadvantage of *in-situ* approach is the excess of graphite powder that impact adversely the specific properties of the MOFs or even destroys the physical structure of MOF [105]. On the other hand, the *ex-situ* approach utilizes the modifier to mix the MOF with the graphite powder, resulting in composite material [106]. The ex-situ approach is reliable since it provides a more accessible and efficient modification of CPE for various electrochemical applications. A simple schematic of an electrochemical approach is shown in Figure 6.

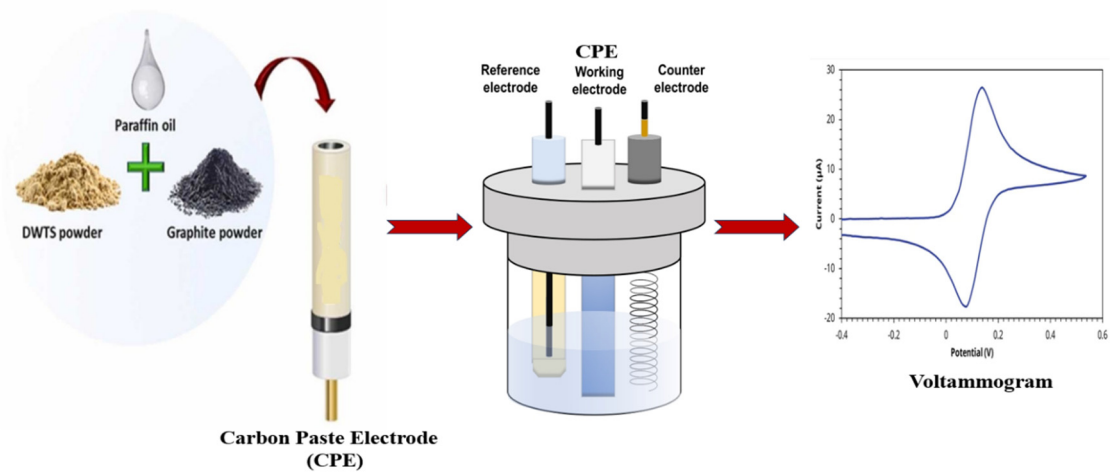

Figure 6. *Ex-situ* fabrication of modified carbon paste electrode and application in the electrochemical detection of analytes.

3.1.2. MOF modified glassy carbon electrode (GCE)

Glassy carbon electrodes showed outstanding physical properties, *viz.*, withstand at higher temperatures, hardness, low density, low electrical resistance, low thermal resistance, extreme chemical resistance, and gas and liquid impermeability. A restrained pyrolysis of phenol-formaldehyde resin in an inert atmosphere produces a glassy carbon electrode. Pyrolysis is the thermal decomposition of an organic precursor or hydrocarbons. Glassy carbon is usually obtained

 doi:10.20944/preprints202309.0192.v1

at a temperature >2000^{0}C since pyrolysis composites have low thermal conduction, resulting in a thermal drop within the sample [107]. On the other hand, the nanoscale fabrication of glassy carbon is achieved relatively at a lower pyrolysis temperature, i.e., Ca. 900^{0}C associated with oxygen impurities [108].

In the fabrication of the working electrode, the glassy carbon electrode was first polished using an alumina slurry on a polishing cloth, followed by the tip of the electrode was dipped in deionized water and ethanol, followed by sonication for 10 min, and the electrode was dried slightly above the room temperature. The modifier (MOF) was mixed with ethanol and then sonicated for 20 min to get a fine mixture of the solution, which was then dropped on the glassy carbon electrode's tip and again dried at ambient temperature. Finally, the Nafion solution was cast on the MOF-modified electrode and dried at ambient temperature [109].

4. Application of MOF in electrochemical sensing

In electrochemical sensors using MOF-modified electrodes in amperometric and voltammetric methods gained attention, particularly for detecting several pharmaceuticals, heavy metals, biomolecules, and other micro-pollutants. The MOF-based sensors showed a significantly low detection limit (LOD) and enhanced selectivity compared to the sensors based on other materials.

4.1. Biomolecules sensing

Biomolecules are the essentials of living organisms that control various biochemical functions of the body. Therefore, the quantitative determination of biomolecules is necessary for chemical pathology or even food chemistry. The electrochemical technique proves to be prominent in quantifying various biomolecules in different matrices [110]. Detecting biomolecules employs different methods; however, the electrochemical methods are promising and show potential in the trace detection of several biomolecules [111].

The electrochemical detection of biomolecules utilizing electrodes fabricated in two ways: i) Enzyme-modified electrodes and ii) Non-Enzymatic or electrodes modified with novel materials (MOF, nanomaterials, metal oxides, etc.). In order to obtain an enhanced selectivity for an analyte, the methods primarily utilize a variety of enzymes to modify the carbon-based electrodes. Nevertheless, enzyme-modified electrodes showed several limitations in the sensing process since some enzymes are often less mobile on the electrode surface and are stable only at specific temperatures and pH levels [112,113]. These limiting factors prompted the use of non-enzymatic modified sensors. The enzyme replaces this electrode type with novel materials, especially MOF, which has an exceptional physicochemical property with high sensitivity and selectivity towards various analytes [103].

The MOFs synthesized using transition metals like Fe^{2+}, Cu^{2+}, Co^{3+}, and Ni^{2+} are promising in the low-level electrochemical detection of several biomolecules *viz*., glucose, ascorbic acid, urea, and H_2O_2 [114]. The detection of glucose is a widely accepted electrochemical method; Cu-MOF@Pt was effectively used to determine glucose in human serum specimens, with excellent recovery and repeatability [115]. The glassy carbon electrode was modified with the nickel-based MOF and employed in cyclic voltammetry (CV) to detect glucose. NiO and Ni/NiO/CNTs display well-defined NiO redox peaks in the absence of glucose and increased peak currents after glucose addition. Furthermore, in the presence and absence of glucose, Ni/NiO/CNTs exhibit significantly greater peak current than NiO, indicating enhanced electrochemical performance. As glucose concentrations rise, the oxidation peak currents rise, with a minor positive shift in peak potential and a drop in the reduction peak currents. This indicates that Ni/NiO/CNTs have outstanding electrocatalytic activity on glucose oxidation. The mechanism involving the oxidation of glucose may be written as [116]:

$$Ni(OH)_2 + OH^- \rightarrow NiOOH + H_2O + e^- \quad (1)$$

$$NiOOH + \text{glucose} \rightarrow Ni(OH)_2 + \text{glucolactone} \quad (2)$$

Preprints (www.preprints.org) | NOT PEER-REVIEWED | Posted: 4 September 2023 doi:10.20944/preprints202309.0192.v1

On the other hand, the copper and nickel MOF-based electrodes were fabricated and utilized in the electrochemical detection of glucose. A redox couple of Cu^{2+}/Cu^{3+} and Ni^{2+}/Ni^{3+} occurs in an alkaline medium, which in turn leads to the oxidation of transition metals used (i.e., copper or nickel) as shown in Equation (1) and Equation (2), which further catalyzes the oxidation of glucose. The reaction mechanism is shown in Figure 7.

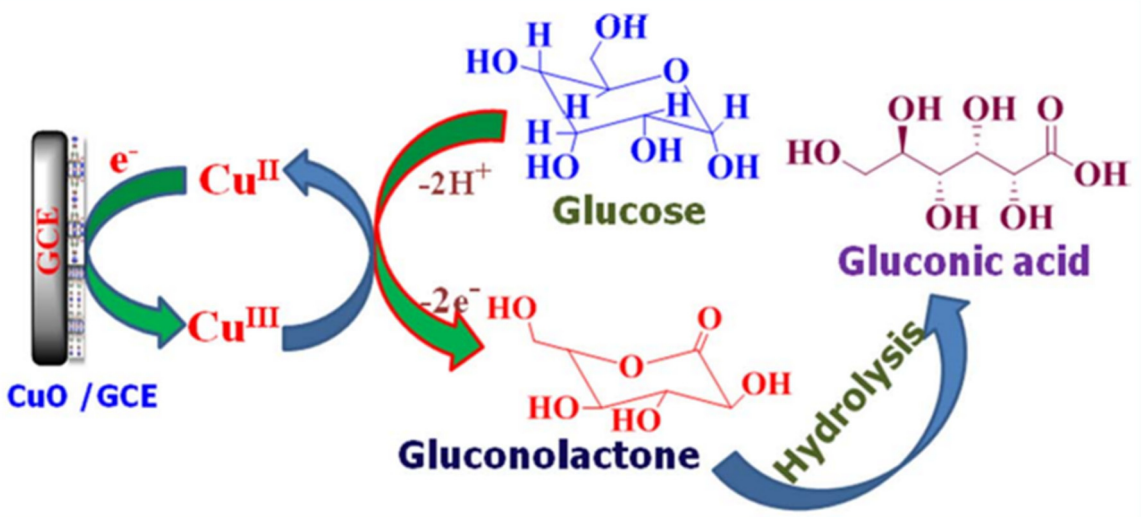

Figure 7. Electrochemical oxidation of glucose on MOF modified GCE [117].

The mechanism of oxidation of glucose on the electrode surface is given as [118,119]:

$$M(OH)_2 + OH^- \rightarrow MOOH + H_2O + e^- \quad (1)$$

$$MOOH + \text{glucose} \rightarrow M(OH)_2 + \text{glucolactone} \quad (2)$$

$$\text{Glucolactone} \quad (\text{Hydrolysis}) \rightarrow \text{Gluconic Acid} \quad (3)$$

The first step oxidizes the M^{2+} to M^{3+}, and these species take part at the electrode surface in glucose oxidation. The most crucial species for glucose oxidation is M^{3+}, which also serves as the primary electron transfer mediator. M^{2+} in the MOF undergoes oxidation to produce M^{3+} throughout the potential scan between 0.3 and 0.5 V. M^{3+} preferentially oxidizes the glucose to produce gluconolactone, which produces gluconic acid by hydrolysis [119]. The Differential pulse voltammogram produced for each 50 µM addition of glucose in 0.1 M NaOH is shown in Figure 8a. Adding of 50 µM glucose to 0.1 M NaOH results in an oxidation peak at +0.38 V. This demonstrates that the GC/CuO electrode is ideal for determining glucose. The amperometric i-t curve for glucose produced at a GC/CuO electrode in 0.1 M NaOH stirred solution at an applied voltage of 0.50 V is shown in Figure 8b. The initial current response of the GC/CuO electrode was due to 5 µM glucose, and the continued addition of 5 µM glucose in each step with a sample interval of 50 sec enhances the current response [117].

Preprints (www.preprints.org) | NOT PEER-REVIEWED | Posted: 4 September 2023 doi:10.20944/preprints202309.0192.v1

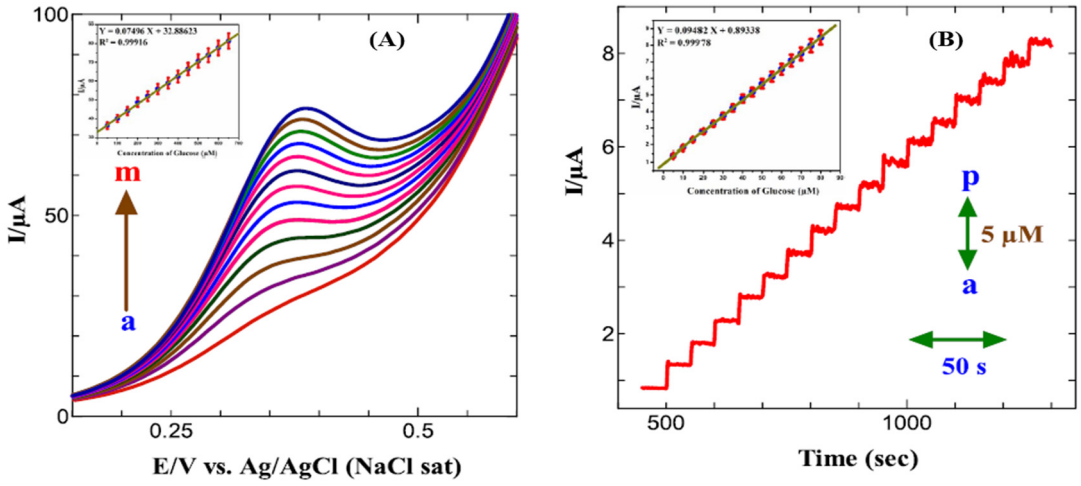

Figure 8. (**a**) The Differential pulse voltammogram produced for each 50 µM addition of glucose in 0.1 M NaOH. (**b**) The amperometric i-t curve for glucose produced at a GC/CuO electrode in 0.1 M NaOH [117].

A chromium-based metal-organic framework (MIL-101) modified with platinum nanoparticles (PtNPs) detects simultaneously the Xanthine, uric acid, and dopamine in spiked serum samples using the differential pulse voltammetry (DPV) [120]. The sensor has an extensive linear range (0.5 - 162 µM), a low detection limit (0.42 µM), and excellent selectivity, according to differential pulse voltammetry. This determines dopamine, uric acid, Xanthine, and hypoxanthine simultaneously at working potentials of 0.13, 0.28, 0.68, and 1.05 V (vs. Ag/AgCl) and to quantify Xanthine in spiked serum samples. DPV curves of simultaneous determination of dopamine (DA), uric acid (UA), Xanthine (XA), and hypoxanthine (HXA) are shown in Figure 9.

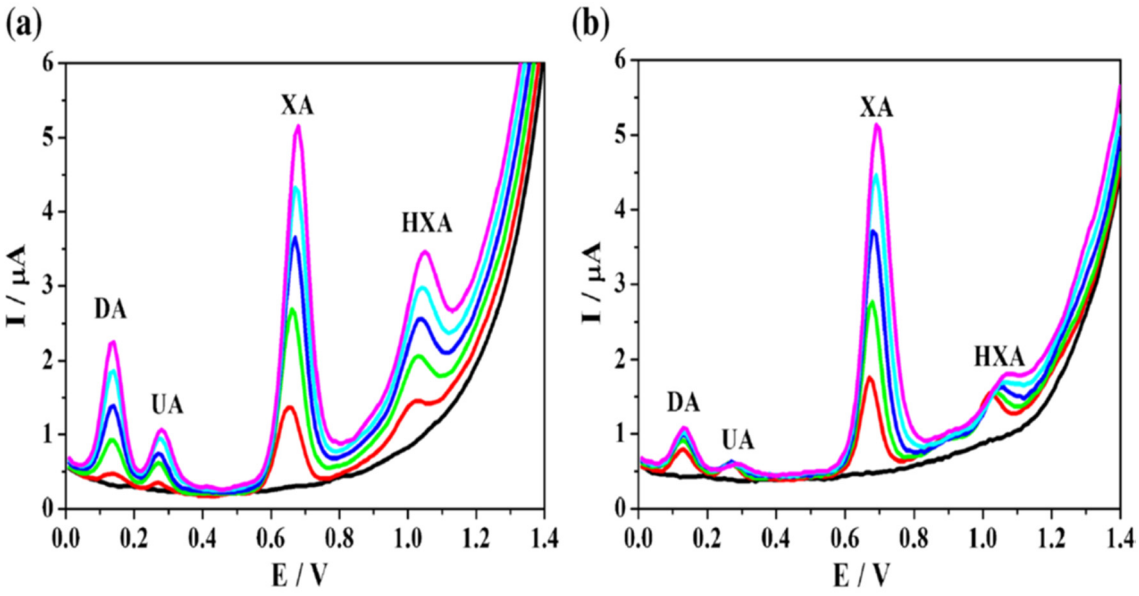

Figure 9. DPV curves of simultaneous determination of (**a**) Xanthine(XA) with different concentration (10, 20, 30, 40, 50 µM) in the presence of 10 µM Dopamine(DA), Uric acid(UA) and Hypoxanthine(HXA) (**b**) Xanthine(XA) with 10µM concentration in the presence of 10 µM Dopamine(DA), Uric acid(UA) and Hypoxanthine(HXA) [114].

Further, Table 2 includes several MOF-based materials used in the electrochemical detection of various biomolecules in real and complex samples. The LOD and Linear range is also included to demonstrate the detection of these biologically important molecules.

Table 2. Electrochemical sensing of several biomolecules using various MOF modified electrodes.

Electrode type	Analyte	MOF	MOF composite	Work potential	pH	LOD	Linear range (10^{-6} mol/L)	Real sample	References
NPCP	Leuteoline	ZIF-67	CuCo@NPCP	0.10V	7.0	0.080 nM	0.20 –2.50	Human vaccine	[121]
G.C.E.	Dopamine	ZIF-8	ZIF-8@G	0.30V	7.0	1.00 μM	3.0 –1.00	Cow vaccine	[122]
G.C.E.	L-Cysteine	HKUST-1	Au-SH-SiO2@Cu-MOF	0.40V	5.0	0.0080 μM	0.02.–300	N/r	[123]
G.C.E.	Ascorbic acid	HKUST-1	HKUST-1@GO	-0.02V	7.0	20.0 nM	0.50–6965	N/r	[91]
G.C.E	Catechol	MIL-101	MIL-101 (Cr)@rGO	N/r	7.0	4.00 μM	10.0–1400	Lake	[103]
G.C.E	Xanthine	MIL-101	Pt-NPs@MIL-101	0.280V	7.0	0.420 μM	0.50–162	Human vaccine	[114]
G.C.E	17β-estradiol	MIL-53	MIP-Pb/MIL-53@CNT	0.210V	3.0	0.00615 pM	0.010–1000	Domestic	[124]
G.C.E	Glucose	GOD/Cu	Hemin	-0.25V	7.0	2.73 μM	9.10-36.0	Human Serum	[125]
G.C.E	Glucose	ZIF-8@GOx	GO	0.4V	7.4	0.05 mM	1-10	Calf Serum	[126]
G.C.E	Glucose	ZIF-8	Fe_3O_4/PPy/GOx	0.6V	7	0.333 μM	1-2	Human Serum	[127]
G.C.E	Glucose	Cu-MOF	MWCNTs	0.55V	7	0.4 μM	0.5-11.84	Human Serum	[128]
G.C.E	Dopamine	UiO-66-NH_2	CNTs	0.0V	7	15nM	0.03-2	Human Serum	[129]
G.C.E	Urea	Ni-MOF	MWCNT/ITO	0.45V		3.0 μM	10-1120	Urine	[130]

doi:10.20944/preprints202309.0192.v1

Preprints (www.preprints.org) | NOT PEER-REVIEWED | Posted: 4 September 2023 doi:10.20944/preprints202309.0192.v1

4.2. Detection of hydrogen peroxide

Hydrogen peroxide (H_2O_2) has physical and chemical significance in different research fields, *viz.*, pharmaceutical industry, food and chemical industry, environment, and biological samples [109,131,132]. In the food industry, bleaching or disinfection utilizes hydrogen peroxide during food processing. However, higher concentrations of hydrogen peroxide residues in food products negatively affect human health. Excessive levels of retained hydrogen peroxide in food showed several harmful effects, which include cancer, rapid aging, coronary artery disease, severe gastrointestinal issues, and neurological illnesses [133]. The necessity of detecting hydrogen peroxide is manifold, and the miniaturized device for *on-site* detection is a prerequisite for various biological or environmental samples. Several detection methods have been employed for many decades. However, the electrochemical methods are promising because of their robustness in operation, selectivity, dependability, and sensitivity towards the analyte, and the on-site detection with a miniaturized device added to the method's suitability [134].

Cobalt-based MOF ($Co(pbda)(4,4\text{-}bpy)\cdot 2H_2O]_n$) was incorporated on GCE and used for the detection of hydrogen peroxide (H_2O_2) at 0.1 M NaOH solution employing cyclic voltammetry (CV) [132]. The cyclic voltammogram of the Co-MOF modified GC electrode exhibits three reduction peaks: (a) in the absence of H_2O_2, (b) with the addition of 0.1 M NaOH solution containing 1 mM H_2O_2 and (c) with the addition of 0.1 M NaOH solution containing 2 mM H_2O_2 at approximately -0.40 V. The amperometric response indicates that the Co-MOF modified GC electrode shows enhanced electrocatalytic response towards the H_2O_2 reduction current, and the calibration line obtains for a wide concentration range of H_2O_2 5 µM to 9.0 mM. The method provides a low detection limit of 3.76 µM and a high sensitivity of 83.10 A μmM^{-1} cm^2 at an applied potential of -0.40 V. Additionally, and the detection method demonstrates favorable selectivity and long-term stability. Furthermore, the mechanism indicated that the Co-MOF is highly efficient in intrinsic peroxidase-like activity, which allows it to catalyze H_2O_2 decomposition to form hydroxyl radical, which then oxidizes the peroxidase substrate (terephthalic acid) to produce colour. Figure 10 shows the reduction of H_2O_2 at an applied potential of -0.4V in the absence of H_2O_2, along with the addition of 0.1M NaOH solution containing 1 and 2 mM H_2O_2. It also depicts the Co-MOF-modified GCE's amperometric response at a potential range of −0.4 to −0.6V [118]. Table 3 comprises the use of different MOFs in the electrochemical detection of hydrogen peroxide in various samples. The limit of detection and experimental conditions with the experimental concentration range of H_2O_2 is included in Table 3.

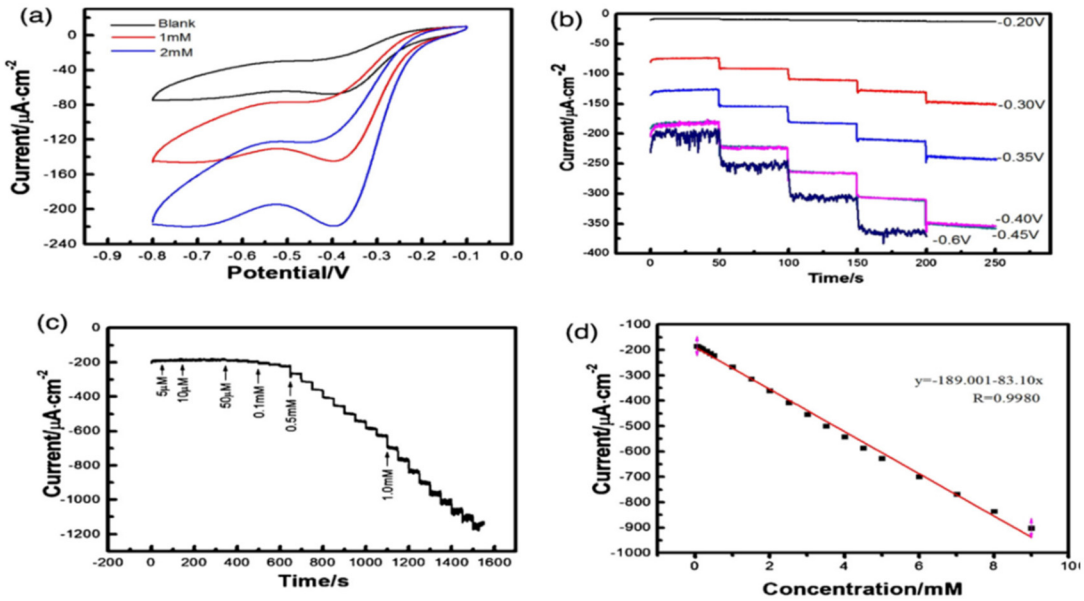

Preprints (www.preprints.org) | NOT PEER-REVIEWED | Posted: 4 September 2023 doi:10.20944/preprints202309.0192.v1

Figure 10. (**a**) Voltammograms and amperometric response of Co-MOF in the absence and presence of 1 and 2 mM H_2O_2 in 0.1 M NaOH solution. (**b**,**c**) Amperometric response of the Co-MOF modified GCE at at potential range −0.4 to −0.6V. (**d**) Calibration curve of Amperometric response [118].

Table 3. MOF-modified carbon-based electrodes used for amperometry measurement of H_2O_2 in various samples.

Electrode type	MOF	Reduction potential	pH	LOD	Linear range (10^{-6} mol/L)	Real sample	Ref.
CPE	Ni-MOF	−0.250 V	13	0.00090 mM	0.0040–60	Cleaning soln.	[135]
GCE	Y1-4-NDC-MOF	−0.50 V	7	0.430 µM	04.0–11000	A549 cells	[136]
GCE	Ce1-xTbx-MOF	0.750 V	7	7.70 µM	0.10 –4.2	N/r	[137]
GCE	[Cu(adp)(BIB)(H2O)]n	N/r	13	0.0680 µM	0.100–2.750	N/r	[138]
GCE	$Cu(btec)_{0.5}DMF$	−0.20 V	6.5	0.8650 µM	5.0–8000	N/r	[139]
GCE	$\{[Cu_2(bep)(ada)_2]H_2O\}_n$	−0.45 V	13	0.014 µM	0.05–3	N/r	[140]
CPE	Cu-MOF	−0.2 V	7.2	1.00 µM	1.0 –0.99	N/r	[141]
GCE	HKUST-1	−0.4 V	7	0.49 µM	1.0–5.6	Raw 264.7 cells	[142]
GCE	Zn-MOF	−0.80 V	7.2	67 nM	1 –5	Milk	[109]
CPE	Co-MOF	−0.30 V	7.2	0.50 µM	1.0–823	N/r	[143]
GCE	MIL-53-Cr(III)	−0.307 V	13	3.520 µM	25.0–500	Human vaccine	[144]
GCE	Ni-MOF/CNTs	0.5V	13	2.1 µM	10-5.600	N/r	[145]
GCE	AuNPs-NH2/Cu-MOF	-0.15V	7.4	1.2 µM	5–850	HeLa cells	[131]
GCE	ZIF-67	-0.05V	7	0.11 µM	1.86-1050	N/r	[146]
GCE	Ag-Bi–BDC (s) MOF	-0.4V	7	0.02 µM	10-5000	THP-1	[147]
GCE	2D Co-MOF	0.25V	12	0.69 µM	0.5-832	N/r	[148]
CPE	AP-Ni-MOF	-0.25V	7	0. 9 µM	4–60000	Lens cleaning solution	[135]

4.3. Organic pollutant sensing

Aromatic organic compounds such as phenol, nitrobenzene, hydrazine, chlorinated phenols, polyaromatic hydrocarbons, pesticides, nitrites, and pharmaceuticals have shown more significant environmental concerns, contaminating the water bodies and severely affecting the human health. The detection and elimination of these pollutants from the aquatic environment has been a concern of environmentalists for the last few decades. Yadav et al. demonstrated the synthesis of zinc (II) based MOF (MOF-5) decorated with the Au(NPs), and the material modifying the glassy carbon electrode and detects the nitrobenzene and nitrite in an aqueous medium [149]. Figure 11(1) shows cyclic voltammograms of nitrite (1.0 mM) using the GC/Au-MOF-5, GC/MOF-5, and GC electrodes in 0.1 M phosphate buffer (PBS) (pH 7.0) at 20 mV/s. An oxidation peak of nitrite appeared at an applied potential of 0.85V using the GC/Au-MOF-5 electrode. However, the reverse scan reveals the reduction peak at 0.46 V.

On the other hand, the nitrite oxidizes at 0.93V and 1.01V using the GC and GC/MOF-5 electrodes, respectively. The results imply a significant increase in peak currents at low applied potentials using the GC/Au-MOF-5 electrode. Therefore, Au(NPs) in Au-MOF-5 showed an efficient electrocatalytic activity for nitrite oxidation. Similarly, the cyclic voltammograms of nitrobenzene (NB) using the GC, GC/MOF-5, and GC/Au-MOF-5 electrodes in an N_2 saturated atmosphere and employing 0.1 M pH 7.0 phosphate buffer, shown in Figure 11(2). In the absence of NB, no peak current appeared in the voltammograms; the presence of NB exhibits a distinct reduction of nitrobenzene, and the reduction peak is observed at an applied potential of -0.77, 0.79, and 0.77 V for the GC, GC/MOF-5 and GC/Au-MOF-5 electrodes, respectively [149].

Preprints (www.preprints.org) | NOT PEER-REVIEWED | Posted: 4 September 2023 doi:10.20944/preprints202309.0192.v1

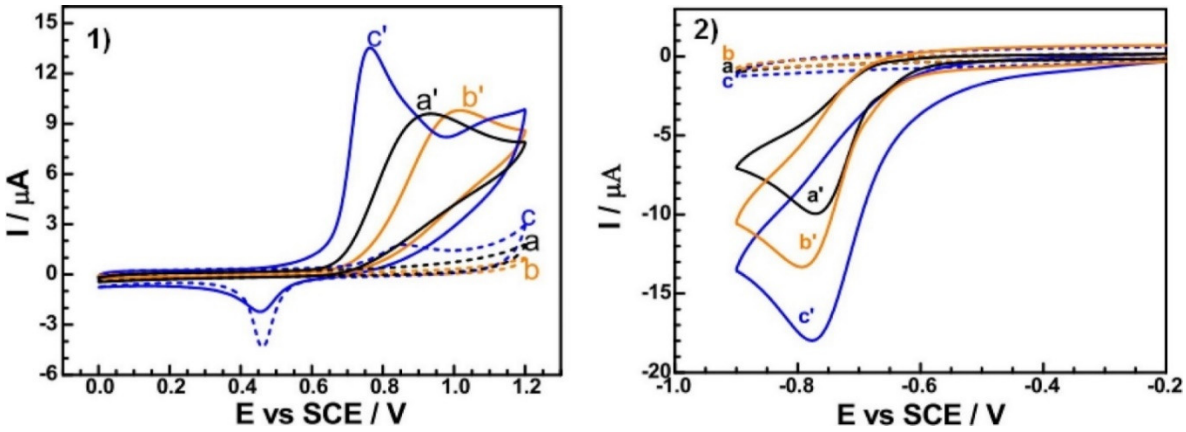

Figure 11. Cyclic Voltammogram of (**1**) Nitrite (**a, b, c** are peaks obtained in the absence of nitrite at 0.1 M PB; **a', b', c'** are peaks obtained in the presence of nitrite at 0.1 M PB) and (**2**) Nitrobenzene (**a, b, c** are peaks obtained in the absence of nitrobenzene at 0.1 M PB; **a', b', c'** are peaks obtained in the presence of nitrobenzene at 0.1 M PB) induced by MOF-5/Au NPs modified GCE [149].

Many nations have limited the use of patulin residues due to their severe toxicity and ubiquitous occurrence in foods. The Meals and Drug Administration of the United States and China mandates a maximum residual of patulin of 50 µM in fruit juice and processing products. In contrast, the European Union mandates a limit of 10 µM in newborn and child meals [150]. Because of the widespread occurrence and high toxicity of patulin in food, a rapid and sensitive detection method averts the possible harmful effects of patulin on human health [132]. Copper-based MOF decorated with the Au(NPs) was used to modify the GCE, which electrochemically detects patulin in apple juice. The square wave voltammograms of patulin show that raising the concentration of patulin from 0.001 nM to 1.0 nM and 1.0 nM to 250.0 nM increased the cathodic signal. The LOQ was 0.001 nM, and the LOD was 3.33 10-4 nM. RSDs of 1.65% and 0.83% were found for six replicate measurements of 1.0 nM and 250.0 nM patulin, respectively [151].

Similarly, the HKUST-1 MOF incorporated with Au(NPs)-GCE detects electrochemically the paracetamol. The MOF/AuNP modified GCE detects the paracetamol efficiently, and a wide linear range of paracetamol concentration (0.01 µM to 100 µM) provides the detection limit of 0.0011 µM [152]. Cu-BTC nanocrystals/CNTs modified GC electrode showed an improved oxidation current for the metformin detection. Peak current demonstrated good linearity with concentrations ranging from 0.5 µM to 25 µM with a detection limit of 0.12 µM under optimal conditions. Further, the detection method implied for the accurate detection of metformin in pharmaceutical samples [153]. The EPC-modified GCE showed good sensitivity and low detection limit (i.e., 2.9 µM) in detecting chloramphenicol residual in honey [154]. Table 4 displays the list of different types of MOFs used to detect organic contaminants.

Table 4. MOFs for detecting organic contaminants in water.

Electrode type	Analyte	MOF	Work potential	pH	LOD	Linear range (10^{-6} mol/L)	Real sample	References
GCE	Nitrobenzene	MOF-5	−0.790 V	7	15.3 μM	20.0–500	N/r	[149]
GCE	Nitrite	MOF-525	0.90 V	8	2.10 μM	20.0–800	N/r	[155]
CPE	Nitrite	Cu-MOF	0.9 V	7.2	30 nM	50 –712	Lake water	[156]
GCE	Hydrazine	$[Co_2(4\text{-ptz})_2(bpp)(N3)_2]_n$	0.20 V	N/r	N/r	5.0–630	N/r	[157]
GCE	Dihydroxybenzene	HKUST-1	N/r	7	0.590 μM	1.0–1000	Domestic	[158]
GCE	Hydroxylamine	MMPF-6	0.350 V	7	0.004 μM	1–20	Domestic	[159]
GCE	BPA	Ce-MOF	0.520 V	7	02.0 nM	0.005–5.00	Milk	[160]
GCE	Paracetamol	HKUST-1	−0.060 V	6	0.01–100 μM	0.01–100.0	Commercial tabs	[152]
GCE	Metformin	HKUST-1	0.6 V	13	5.0–25 μM	5–25.0	Commercial tabs	[153]
GCE	Chloramphenicol	IRMOF-8	−0.10 V	7.5	0.010–1.0 μM	0.01–1.0	Honey	[154]
GCE	Diphenylether	MAC-ZIF-8	-0.4V	7	0.46 Mm	0-114	Apricot	[161]
GE	Ochratoxin A	AgPt/PCN-223-Fe	-0.6V	6	20-2000	14	Red wine	[162]
GCE	Paraoxon	Ce/UiO-66@MWCNTs	0.2V	7.5	0.01-150	0.004	Spinach	[163]

doi:10.20944/preprints202309.0192.v1

Preprints (www.preprints.org) | NOT PEER-REVIEWED | Posted: 4 September 2023 doi:10.20944/preprints202309.0192.v1

4.4. Heavy metals sensing

Heavy metals such as lead, mercury, cadmium, chromium, and arsenic are potential heavy metals and seriously threaten human health and the marine environment [164]. These heavy metals contaminate the environment due to many geological and human-caused phenomena, including agricultural, industrial, and domestic wastes [165]. The detection of heavy metals in different environmental matrices using various MOF-based sensors has recently gained attention [144]. Although various detection techniques have been developed in the past, electrochemical analysis is one of the prominent and robust techniques due to its accuracy and reliability. The exceptional features of MOF, i.e., high porosity, homogeneous structures, large surface area, and ease of functionalization, received greater attention in the efficient and selective use in sensor developments for detecting several heavy metals [166]. Many MOFs show low conductivity due to the bulk organic linkers coordinated to the core metal atom [167]. Therefore, MOFs are typically coupled with high-conductivity elements such as metal oxides, metal nanoparticles, and carbon compounds to overcome the limitations. Furthermore, MOFs with high conductivity are utilized as alternative materials for the trace detection of several heavy metal toxic ions. Moreover, the repeatability of the signal due to the micro-sized MOFs is one of the challenges in the detection system [14,168,169].

Cd^{2+} and Pb^{2+} were simultaneously and selectively detected in water samples using the Yb-MOF-modified electrode [170]. Under ideal circumstances, the Yb-MOF/GCE electrode detects the Cd^{2+} and Pb^{2+} independently at values ranging from 0 to 40 ppb. I (μA) = 0.2045 x C (ppb) - 0.0838 (Cd^{2+}) and I (μA) = 0.1971 x C (ppb) + 0.0686 (Pb^{2+}) are the recorded current responses on DPASV curves that grow linearly with increasing ion concentration. For Cd^{2+} and Pb^{2+}, the detection limits (LOD) were 7.40 ppb and 2.02 ppb, respectively. The use of Yb-MOF/GCE for the simultaneous electrochemical detection of Cd^{2+} and Pb^{2+} in the concentration range of 0 to 50 ppb. I (μA) = 0.4676 x C (ppb) + 0.0414 (R^2 = 0.997) for Cd^{2+} and I (μA) = 0.4082 x C (ppb) - 0.26 (R^2 = 0.998) for Pb^{2+}, as shown in Figure 12, increased linearly with the ion concentrations. For Cd^{2+} and Pb^{2+}, the sensitivities were 469 μA ppm^{-1} cm^{-2} and 397 μA ppm^{-1} cm^{-2}, respectively. The detection limits for Cd^{2+} and Pb^{2+} were 3.0 ppb and 1.6 ppb, respectively. Pb^{2+} was more favorably absorbed and reduced on the porous structure of the Yb-MOF framework than Cd^{2+} [171]. The recent advancements in the electrochemical detection of heavy metals using MOFs are illustrated in Table 5, along with the optimized pH and potential.

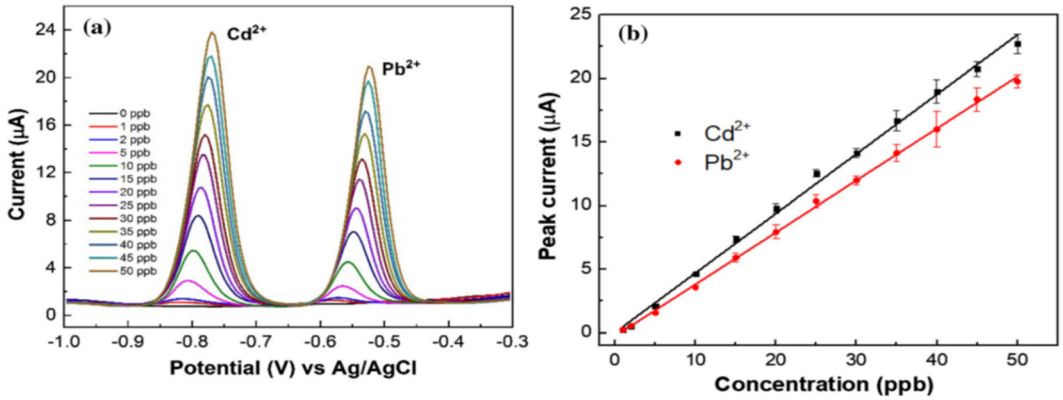

Figure 12. (**a**) The simultaneous voltammograms of Cd^{2+} and Pb^{2+} (**b**) the corresponding calibration curve using Ytterbium-based MOF [148].

Table 5. Examples of carbon-based electrodes modified with MOFs for measuring the concentration of heavy metals in water using stripping voltammetry.

Electrode Type	Analyte	M.O.F	Penetration potential	pH	L.O.D	Linear Range (10^{-6} mol/L)	Real sample	Ref
CPE	Cd^{2+}	$[Zn2(NH2\text{-}BDC)_2(4\text{-}bpdh)]\cdot 3DMF$	-1.0V	3	0.2 µM	0.7 – 120	Tap water	[172]
GCE	Zn^{2+}	BiCux-ANPs@CF/SPCE	-1.2V	4.5	35 µM	150-600	Urine	[173]
CPE	Pb^{2+}	MOF-5	-0.9V	5	4.9 µM	10 – 1000	Tap water	[174]
GCE	Hg^{2+}	$3DGO/UiO\text{-}66\text{-}NH_2$	-1.1V	7.4	3.1 µM	0.01-3.5	Rice and honey sample	[175]
GCE	Cu^{2+}	Co-TMC4R-BDC	-1.3V	5	0.067 µM	0.25-9	Lake water	[176]
GCE	Cu^{2+}	Yb-MOF	-1.1V	4.5	1.6 µM	0-50	River water	[171]
GCE	Hg^{2+}	UiO-66-NH2/GaOOH	-1.0V	6	0.006 µM	0.10-0.45	Waste water	[177]
GCE	Pb^{2+}	$NH_2\text{-}CU_3(BTC)_2$	-1.0V	4.5	5.0 µM	10 – 500	Powder milk	[178]
GCE	Hg^{2+}	Fe1Co1	-1.0V	5	0.0078 µM	0.1-1.1	River water	[179]
CPE	Cu^{2+}	MIL -47	-1.10V	4.5	0.087 µM	1-10	Lake water	[180]
GCE	Hg^{2+}	ZJU -27	-0.58V	5	0.0013 µM	0.5-2	Lake water	[94]
GCE	Pb^{2+}	ZIF-8	-1.2V	4.7	4.16 µM	12 – 100	N/R	[181]
GCE	Cu^{2+}	$GA\text{-}UiO\text{-}66\text{-}NH_2$	-1.3V	5	0.008 µM	0.01-1.6	Vegetable	[182]
GPE	Cu^{2+}	Ca -MOF	-0.2V	4.5	1.4 µM	10-60	Waste water	[183]
GCE	Hg^{2+}	ZIF -67/EG	-0.80V	5	0.00129 µM	0.5-3	Waste water	[184]
CPE	Pb^{2+}	MOF-235	N/r	N/r	50 µM	N/r	Tap water	[96]
KSC	Hg^{2+}	Zr -DMBD MOF	-0.8V	6	0.05 µM	0.25-3.5	River water	[185]

doi:10.20944/preprints202309.0192.v1

 doi:10.20944/preprints202309.0192.v1

5. Conclusion and Future perspective

MOFs and MOF-derived materials are suitable modifiers of electrodes for detecting different pollutants in aquatic environments. MOFs possess distinctive properties such as high specific surface area, pore working capabilities, and regulated shape and size of pores. Moreover, using suitable organic linkers in the material synthesis makes the material a flexible framework for the target adsorbate ions/molecules. Therefore, ample opportunities lie for advancement in the development of MOFs-based sensing devices by improving the sensitivity and stability of the material. Further study on developing MOF and MOF-derived materials for practical applications could open newer avenues for sensing in environmental applications.

Several researchers reported ground-breaking achievements in the applications of MOFs for electrochemical sensors in the recent past; however, advancements towards the MOFs developments for targeted sensors applications. Compared to carbon-based materials, MOF-derived composites face lesser sensitivities, poor stability, and less repeatability. Therefore, synthesizing advanced MOFs materials could enable viable alternatives for miniaturized device development. Similarly, there are several challenges in the development of sensors using MOF and MOF-based materials; the following are the critical issues of employing MOF-based materials in electrochemical sensors:

i. Challenges encompass the synthesis of advanced materials to control the shape and size of MOFs; this may result in uniform growth of nanostructures with a significant increase in surface area.
ii. Homogeneous dispersion of active metals on the surface of MOF-derived carbons remains challenging.
iii. Although many MOFs are used to fabricate electrodes for heavy metal detection, the insights into electrochemical sensing mechanisms could enable greater implications for device development.
iv. MOF stability in an aqueous media remains challenging; studies on coupling hydrophobic ligands with high valence metal ions could provide newer research areas for suitable applications.
v. Since MOFs' pore width and geometry play an essential role in the highly selective determination of food contaminants, synthesizing functionalized MOFs could enable required selectivity towards the target analyte species in complex matrices.

References

1. Wiśniewska, P.; Haponiuk, J.; Saeb, M.R.; Rabiee, N.; Bencherif, S.A. Mitigating Metal-Organic Framework (MOF) Toxicity for Biomedical Applications. *Chem. Eng. J.* **2023**, *471*, 144400.
2. Ettlinger, R.; Lächelt, U.; Gref, R.; Horcajada, P.; Lammers, T.; Serre, C.; Couvreur, P.; Morris, R.E.; Wuttke, S. Toxicity of Metal–Organic Framework Nanoparticles: From Essential Analyses to Potential Applications. *Chem. Soc. Rev.* **2022**, *51*, 464–484.
3. Fan, W.; Yuan, S.; Wang, W.; Feng, L.; Liu, X.; Zhang, X.; Wang, X.; Kang, Z.; Dai, F.; Yuan, D.; et al. Optimizing Multivariate Metal–Organic Frameworks for Efficient C2H2/CO2 Separation. *J. Am. Chem. Soc.* **2020**, *142*, 8728–8737.
4. Herbst, A.; Janiak, C. MOF Catalysts in Biomass Upgrading towards Value-Added Fine Chemicals. *Cryst. Eng. Comm* **2017**, *19*, 4092–4117.
5. Pornea, A.M.; Kim, H. Synthesis of Hybrid Dual-MOF Encapsulated Phase-Changing Material for Improved Broadband Light Absorption and Photothermal Conversion Enabling Efficient Solar Energy Storage. *Sol. Ene. Mat and Sol. Cells.* **2022**, *244*, 111817.
6. Dong, Z.; Sun, Y.; Chu, J.; Zhang, X.; Deng, H. Multivariate Metal–Organic Frameworks for Dialing-in the Binding and Programming the Release of Drug Molecules. *J. Am. Chem. Soc.* **2017**, *139*, 14209–14216.
7. Tchalala, M.R.; Bhatt, P.M.; Chappanda, K.N.; Tavares, S.R.; Adil, K.; Belmabkhout, Y.; Shkurenko, A.; Cadiau, A.; Heymans, N.; De Weireld, G.; et al. Fluorinated MOF Platform for Selective Removal and Sensing of SO 2 from Flue Gas and Air. *Nat. Com.* **2019**, *10*.

8. Kannangara, Y.Y.; Rathnayake, U.A.; Song, J.-K. Redox Active Multi-Layered Zn-PPDA MOFs as High-Performance Supercapacitor Electrode Material. *Electrochem. Acta*. **2019**, *297*, 145–154.
9. Li, H.; Eddaoudi, M.; O'Keeffe, M.; Yaghi, O.M. Design and Synthesis of an Exceptionally Stable and Highly Porous Metal-Organic Framework. *Nature.* **1999**, *402*, 276–279.
10. Sohrabi, H.; Ghasemzadeh, S.; Ghoreishi, Z.; Majidi, M.R.; Yoon, Y.; Dizge, N.; Khataee, A. Metal-Organic Frameworks (MOF)-Based Sensors for Detection of Toxic Gases: A Review of Current Status and Future Prospects. *Mat. Chem. and Phy.* **2023**, *299*, 127512.
11. Chui, S.S.-Y.; Lo, S.M.-F.; Charmant, J.P.H.; Orpen, A.G.; Williams, I.D. A Chemically Functionalizable Nanoporous Material [Cu3(TMA)2(H2O)3]n. *Science* **1999**, *283*, 1148–1150.
12. Devic, T.; Serre, C. High Valence 3p and Transition Metal Based MOFs. *Chem. Soc. Rev.* **2014**, *43*, 6097–6115.
13. Loiseau, T.; Volkringer, C.; Haouas, M.; Taulelle, F.; Férey, G. Crystal Chemistry of Aluminium Carboxylates: From Molecular Species towards Porous Infinite Three-Dimensional Networks. *Comptes Rendus Chimie* **2015**, *18*, 1350–1369.
14. Cao, Y.; Wang, L.; Shen, C.; Wang, C.; Hu, X.; Wang, G. An Electrochemical Sensor on the Hierarchically Porous Cu-BTC MOF Platform for Glyphosate Determination. *Sens. and Act. B: Chemical* **2019**, *283*, 487–494.
15. Rana, A.; Baig, N.; Saleh, T.A. Electrochemically Pretreated Carbon Electrodes and Their Electroanalytical Applications – A Review. *Jou.l of Electroanal. Chem.* **2019**, *833*, 313–332.
16. Rupam, T.; Palash, M.L.; Jahan, I.; Harish, S.; Saha, B. *GREEN SYNTHESIS AND ADSORPTION CHARACTERISATION OF AN ALUMINIUM BASED METAL ORGANIC FRAMEWORK*; **2019**;
17. Hu, C.; Xiao, J.-D.; Mao, X.-D.; Song, L.-L.; Yang, X.-Y.; Liu, S.-J. Toughening Mechanisms of Epoxy Resin Using Aminated Metal-Organic Framework as Additive. *Mat. Let.* **2019**, *240*, 113–116.
18. Hu, Z.; Wang, Y.; Zhao, D. Modulated Hydrothermal Chemistry of Metal–Organic Frameworks. *Acc. Mater. Res.* **2022**, *3*, 1106–1114.
19. Abdelkareem, M.A.; Abbas, Qaisar.; Mouselly, M.; Alawadhi, H.; Olabi, A.G. High-Performance Effective Metal–Organic Frameworks for Electrochemical Applications. *Jou. of Sc: Adv. Mat. and Dev.* **2022**, *7*, 100465.
20. Liu, B.; Vellingiri, K.; Jo, S.-H.; Kumar, P.; Ok, Y.S.; Kim, K.-H. Recent Advances in Controlled Modification of the Size and Morphology of Metal-Organic Frameworks. *Nano Res.* **2018**, *11*, 4441–4467.
21. Yaghi, O.M.; Li, H. Hydrothermal Synthesis of a Metal-Organic Framework Containing Large Rectangular Channels. *Jou. of the Amer. Chem. Soc.* **1995**, *117*, 10401–10402.
22. Qi, Y.; Luo, F.; Che, Y.; Zheng, J. Hydrothermal Synthesis of Metal-Organic Frameworks Based on Aromatic Polycarboxylate and Flexible Bis(Imidazole) Ligands. *Crys. Grow. and Des.* **2008**, *8*, 606–611.
23. Horcajada, P.; Surblé, S.; Serre, C.; Hong, D.-Y.; Seo, Y.-K.; Chang, J.-S.; Grenèche, J.-M.; Margiolaki, I.; Férey, G. Synthesis and Catalytic Properties of MIL-100(Fe), an Iron(III) Carboxylate with Large Pores. *Chem. Com.* **2007**, 2820–2822.
24. Chen, L.; Guo, H.; Fujita, T.; Hirata, A.; Zhang, W.; Inoue, A.; Chen, M. Nanoporous PdNi Bimetallic Catalyst with Enhanced Electrocatalytic Performances for Electro-Oxidation and Oxygen Reduction Reactions. *Adv. Funct. Mat.* **2011**, *21*, 4364–4370.
25. Wu, H.; Li, M.; Wang, Z.; Yu, H.; Han, J.; Xie, G.; Chen, S. Highly Stable Ni-MOF Comprising Triphenylamine Moieties as a High-Performance Redox Indicator for Sensitive Aptasensor Construction. *Analytica Chimica Acta* **2019**, *1049*, 74–81.
26. Liu, X.; Yang, H.; Diao, Y.; He, Q.; Lu, C.; Singh, A.; Kumar, A.; Liu, J.; Lan, Q. Recent Advances in the Electrochemical Applications of Ni-Based Metal Organic Frameworks (Ni-MOFs) and Their Derivatives. *Chemosphere* **2022**, *307*, 135729.
27. Ahmadi, A.; Nezamzadeh-Ejhieh, A. A Comprehensive Study on Electrocatalytic Current of Urea Oxidation by Modified Carbon Paste Electrode with Ni(II)-Clinoptilolite Nanoparticles: Experimental Design by Response Surface Methodology. *J. Electroanal. chem.* **2017**, *801*, 328–337.
28. Pourtaheri, A.; Nezamzadeh-Ejhieh, A. Enhancement in Photocatalytic Activity of NiO by Supporting onto an Iranian Clinoptilolite Nano-Particles of Aqueous Solution of Cefuroxime Pharmaceutical Capsule. *Spectrochimica Acta - Part A: Molecular and Biomolecular Spectroscopy* **2015**, *137*, 338–344.
29. Sheikh-Mohseni, M.H.; Nezamzadeh-Ejhieh, A. Modification of Carbon Paste Electrode with Ni-Clinoptilolite Nanoparticles for Electrocatalytic Oxidation of Methanol. *Electrochimica Acta* **2014**, *147*, 572–581.

30. Liu, Y.; Myers, E.J.; Rydahl, S.A.; Wang, X. Ultrasonic-Assisted Synthesis, Characterization, and Application of a Metal–Organic Framework: A Green General Chemistry Laboratory Project. *J. Chem. Educ.* **2019**, *96*, 2286–2291.
31. Vinoth, V.; Wu, J.J.; Asiri, A.M.; Anandan, S. Sonochemical Synthesis of Silver Nanoparticles Anchored Reduced Graphene Oxide Nanosheets for Selective and Sensitive Detection of Glutathione. *Ultrason. Sonochem.* **2017**, *39*, 363–373.
32. Areerob, Y.; Cho, J.Y.; Jang, W.K.; Oh, W.-C. Enhanced Sonocatalytic Degradation of Organic Dyes from Aqueous Solutions by Novel Synthesis of Mesoporous Fe3O4-Graphene/ZnO@SiO2 Nanocomposites. *Ultrason. Sonochem.* **2018**, *41*, 267–278.
33. Qiu, L.-G.; Li, Z.-Q.; Wu, Y.; Wang, W.; Xu, T.; Jiang, X. Facile Synthesis of Nanocrystals of a Microporous Metal–Organic Framework by an Ultrasonic Method and Selective Sensing of Organoamines. *Chem. Commun.* **2008**, 3642–3644.
34. Khan, N.A.; Jhung, S.H. Facile Syntheses of Metal-Organic Framework Cu3(BTC)2(H2O)3 under Ultrasound. *Bulletin of the Korean Chem. Soc.* **2009**, *30*, 2921–2926.
35. He, S.; Wu, L.; Li, X.; Sun, H.; Xiong, T.; Liu, J.; Huang, C.; Xu, H.; Sun, H.; Chen, W.; et al. Metal-Organic Frameworks for Advanced Drug Delivery. *Acta Pharmaceutica Sinica B* **2021**, *11*, 2362–2395.
36. Taghipour, A.; Rahimpour, A.; Rastgar, M.; Sadrzadeh, M. Ultrasonically Synthesized MOFs for Modification of Polymeric Membranes: A Critical Review. *Ultrason. Sonochem.* **2022**, *90*, 106202.
37. Iron-Based Metal-Organic Framework: Synthesis, Structure and Current Technologies for Water Reclamation with Deep Insight into Framework Integrity. *Chemosphere* **2021**, *284*, 131171.
38. Ge, J.; Wu, Z.; Huang, X.; Ding, M. An Effective Microwave-Assisted Synthesis of MOF235 with Excellent Adsorption of Acid Chrome Blue K. *J.l of Nanomat.* **2019**, *2019*, e4035075.
39. Ahn, W.S.; Kang, K.K.; Kim, K.Y. Synthesis of TS-1 by Microwave Heating of Template-Impregnated SiO2–TiO2 Xerogels. *Catalysis Letters.* **2001**, *72*, 229–232.
40. Jin, T.; Hwang, Y.K.; Hong, D.-Y.; Jhung, S.H.; Hwang, J.-S.; Park, S.-E.; Kim, Y.H.; Chang, J.-S. Microwave Synthesis, Characterization and Catalytic Properties of Titanium-Incorporated ZSM-5 Zeolite. *Res Chem Intermed* **2007**, *33*, 501–512.
41. Komarneni, S.; Rajha, R.K.; Katsuki, H. Microwave-Hydrothermal Processing of Titanium Dioxide1Dedicated to Professor Shigeyuki Somiya.1. *Mater. Chem. and Phys.* **1999**, *61*, 50–54.
42. Tompsett, G.A.; Conner, W.C.; Yngvesson, K.S. Microwave Synthesis of Nanoporous Materials. *Chemphyschem*. **2006**, *7*, 296–319.
43. Haque, E.; Khan, N.A.; Kim, C.M.; Jhung, S.H. Syntheses of Metal–Organic Frameworks and Aluminophosphates under Microwave Heating: Quantitative Analysis of Accelerations. *Crystal Growth & Design* **2011**, *11*, 4413–4421.
44. Ni, Z.; Masel, R.I. Rapid Production of Metal–Organic Frameworks via Microwave-Assisted Solvothermal Synthesis. *J. Am. Chem. Soc.* **2006**, *128*, 12394–1239.
45. Parnham, E.R.; Morris, R.E. Ionothermal Synthesis of Zeolites, Metal–Organic Frameworks, and Inorganic–Organic Hybrids. *Acc. Chem. Res.* **2007**, *40*, 1005–1013.
46. Choi, J.-S.; Son, W.-J.; Kim, J.; Ahn, W.-S. Metal–Organic Framework MOF-5 Prepared by Microwave Heating: Factors to Be Considered. *Microporous and Mesoporous Mater.* **2008**, *116*, 727–731.
47. Liu, H.; Zhao, Y.; Zhou, C.; Mu, B.; Chen, L. Microwave-Assisted Synthesis of Zr-Based Metal–Organic Framework (Zr-Fum-Fcu-MOF) for Gas Adsorption Separation. *Chem. Phys. Let.* **2021**, *780*, 138906.
48. Ameloot, R.; Stappers, L.; Fransaer, J.; Alaerts, L.; Sels, B.F.; De Vos, D.E. Patterned Growth of Metal-Organic Framework Coatings by Electrochemical Synthesis. *Chem. Mater.* **2009**, *21*, 2580–2582.
49. Bétard, A.; Fischer, R.A. Metal–Organic Framework Thin Films: From Fundamentals to Applications. *Chem. Rev.* **2012**, *112*, 1055–1083.
50. Al-Kutubi, H.; Dikhtiarenko, A.; Zafarani, H.R.; Sudhölter, E.J.R.; Gascon, J.; Rassaei, L. Facile Formation of ZIF-8 Thin Films on ZnO Nanorods. *CrystEngComm.* **2015**, *17*, 5360–5364.
51. Asghar, A.; Iqbal, N.; Noor, T.; Kariuki, B.M.; Kidwell, L.; Easun, T.L. Efficient Electrochemical Synthesis of a Manganese-Based Metal–Organic Framework for H2 and CO2 Uptake. *Green Chem.* **2021**, *23*, 1220–1227.
52. Guerrero, V.V.; Yoo, Y.; McCarthy, M.C.; Jeong, H.-K. HKUST-1 Membranes on Porous Supports Using Secondary Growth. *J. of Mat. Chem.* **2010**, *20*, 3938–3943.

53. Neto, O.J. de L.; Frós, A.C. de O.; Barros, B.S.; Monteiro, A.F. de F.; Kulesza, J. Rapid and Efficient Electrochemical Synthesis of a Zinc-Based Nano-MOF for Ibuprofen Adsorption. *New J. Chem.* **2019**, *43*, 5518–5524.
54. Li, W.-J.; Lü, J.; Gao, S.-Y.; Li, Q.-H.; Cao, R. Electrochemical Preparation of Metal–Organic Framework Films for Fast Detection of Nitro Explosives. *J. Mater. Chem. A* **2014**, *2*, 19473–19478.
55. Nadizadeh, Z.; Naimi-Jamal, M.R.; Panahi, L. Mechanochemical Solvent-Free in Situ Synthesis of Drug-Loaded {Cu2(1,4-Bdc)2(Dabco)}n MOFs for Controlled Drug Delivery. *J. of Solid State Chem.* **2018**, *259*, 35–42.
56. Tanaka, S. Chapter 10 - Mechanochemical Synthesis of MOFs. In *Metal-Organic Frameworks for Biomedical Applications*; Mozafari, M., Ed.; Woodhead Publishing. **2020**; pp. 197–222.
57. Friščić, T. Supramolecular Concepts and New Techniques in Mechanochemistry: Cocrystals, Cages, Rotaxanes, Open Metal–Organic Frameworks. *Chem. Soc. Rev.* **2012**, *41*, 3493–3510.
58. Lv, D.; Chen, Y.; Li, Y.; Shi, R.; Wu, H.; Sun, X.; Xiao, J.; Xi, H.; Xia, Q.; Li, Z. Efficient Mechanochemical Synthesis of MOF-5 for Linear Alkanes Adsorption. *J. of Chem. and Eng. Data.* **2017**, *62*, 2030–2036.
59. Kaur, G.; Anthwal, A.; Kandwal, P.; Sud, D. Mechanochemical Synthesis and Theoretical Investigations of Fe (II) Based MOF Containing 4,4′-Bipyridine with Ordained Intercalated p-Aminobenzoic Acid: Application as Fluoroprobe for Detection of Carbonyl Group. *Inorganica Chimica Acta.* **2023**, *545*, 121248.
60. Prochowicz, D.; Sokołowski, K.; Justyniak, I.; Kornowicz, A.; Fairen-Jimenez, D.; Friščić, T.; Lewiński, J. A Mechanochemical Strategy for IRMOF Assembly Based on Pre-Designed Oxo-Zinc Precursors. *Chem. Commun.* **2015**, *51*, 4032–4035.
61. Kujawa, J.; Al-Gharabli, S.; Muzioł, T.M.; Knozowska, K.; Li, G.; Dumée, L.F.; Kujawski, W. Crystalline Porous Frameworks as Nano-Enhancers for Membrane Liquid Separation – Recent Developments. *Coordin. Chem. Rev.* **2021**, *440*, 213969.
62. Mu, X.; Jiang, J.; Chao, F.; Lou, Y.; Chen, J. Ligand Modification of UiO-66 with an Unusual Visible Light Photocatalytic Behavior for RhB Degradation. *Dalton Trans.* **2018**, *47*, 1895–1902.
63. Srinivasan, R.; Elaiyappillai, E.; Nixon, E.J.; Sharmila Lydia, I.; Johnson, P.M. Enhanced Electrochemical Behaviour of Co-MOF/PANI Composite Electrode for Supercapacitors. *Inorganica Chimica Acta.* **2020**, *502*, 119393.
64. Li, N.; Li, Y.; Li, Q.; Zhao, Y.; Liu, C.-S.; Pang, H. NiO Nanoparticles Decorated Hexagonal Nickel-Based Metal-Organic Framework: Self-Template Synthesis and Its Application in Electrochemical Energy Storage. *J. Colloid. Interface Sci.* **2021**, *581*, 709–718.
65. Ouyang, B.; Chen, Q.; Yuan, H.; Hu, R.; Liang, C.; Liu, F.; Pan, L.; Zhang, Y.; Wu, X.; Yang, S.-T. Reversible Environmental Impacts of Iron-Based Metal-Organic Framework MIL-53(Fe) on Nitrogen-Fixing Bacterium Azotobacter Vinelandii. *J.Env. Chem. Eng.* **2022**, *10*, 107794.
66. Pu, C.; Zhao, H.; Hong, Y.; Zhan, Q.; Lan, M. Elution-Free Ultra-Sensitive Enrichment for Glycopeptides Analyses: Using a Degradable, Post-Modified Ce-Metal–Organic Framework. *Analytica Chimica Acta* **2019**, *1045*, 123–131.
67. Rezki, M.; Septiani, N.L.W.; Iqbal, M.; Harimurti, S.; Sambegoro, P.; Adhika, D.R.; Yuliarto, B. Amine-Functionalized Cu-MOF Nanospheres towards Label-Free Hepatitis B Surface Antigen Electrochemical Immunosensors. *J. Mater. Chem. B* **2021**, *9*, 5711–5721.
68. Yin, Y.; Shao, J.; Zhang, L.; Cui, Q.; Wang, H. Study on Heat Conduction and Adsorption/Desorption Characteristic of MIL-101/Few Layer Graphene Composite. *J Porous Mater* **2021**, *28*, 1197–1213.
69. Burgaz, E.; Erciyes, A.; Andac, M.; Andac, O. Synthesis and Characterization of Nano-Sized Metal Organic Framework-5 (MOF-5) by Using Consecutive Combination of Ultrasound and Microwave Irradiation Methods. *Inorganica Chimica Acta* **2019**, *485*, 118–124.
70. Cho, H.-Y.; Kim, J.; Kim, S.-N.; Ahn, W.-S. High Yield 1-L Scale Synthesis of ZIF-8 via a Sonochemical Route. *Microporous and Mesoporous Materials* **2013**, *169*, 180–184.
71. Yang, D.-A.; Cho, H.-Y.; Kim, J.; Yang, S.-T.; Ahn, W.-S. CO2 Capture and Conversion Using Mg-MOF-74 Prepared by a Sonochemical Method. *Energy Environ. Sci.* **2012**, *5*, 6465–6473.
72. Brainer, N.S.; dos Santos, T.V.; D.E.S. Barbosa, C.; Meneghetti, S.M.P. Simple and Fast Ultrasound-Assisted Synthesis of Sn-MOFs and Obtention of SnO2. *Materials Letters.* **2020**, *280*, 128512.
73. Azad, F.N.; Ghaedi, M.; Dashtian, K.; Hajati, S.; Pezeshkpour, V. Ultrasonically Assisted Hydrothermal Synthesis of Activated Carbon–HKUST-1-MOF Hybrid for Efficient Simultaneous Ultrasound-Assisted

Removal of Ternary Organic Dyes and Antibacterial Investigation: Taguchi Optimization. *Ultrasonics Sonochem.* **2016**, *31*, 383–393.

74. Wu, X.; Bao, Z.; Yuan, B.; Wang, J.; Sun, Y.; Luo, H.; Deng, S. Microwave Synthesis and Characterization of MOF-74 (M=Ni, Mg) for Gas Separation. *Microporous and Mesoporous Materials.* **2013**, *180*, 114–122.
75. Yoo, Y.; Lai, Z.; Jeong, H.-K. Fabrication of MOF-5 Membranes Using Microwave-Induced Rapid Seeding and Solvothermal Secondary Growth. *Microporous and Mesoporous Materials.* **2009**, *123*, 100–106.
76. Jung, D.-W.; Yang, D.-A.; Kim, J.; Kim, J.; Ahn, W.-S. Facile Synthesis of MOF-177 by a Sonochemical Method Using 1-Methyl-2-Pyrrolidinone as a Solvent. *Dalton Trans.* **2010**, *39*, 2883–2887.
77. Minh, T.T.; Phong, N.H.; Van Duc, H.; Khieu, D.Q. Microwave Synthesis and Voltammetric Simultaneous Determination of Paracetamol and Caffeine Using an MOF-199-Based Electrode. *J Mater Sci* **2018**, *53*, 2453–2471.
78. Han, Y.; Cui, J.; Yu, Y.; Chao, Y.; Li, D.; Wang, C.; Wallace, G.G. Efficient Metal-Oriented Electrodeposition of a Co-Based Metal-Organic Framework with Superior Capacitive Performance. *Chem. Sus. Chem.* **2022**, *15*, e202200644.
79. Worrall, S.D.; Bissett, M.A.; Hill, P.I.; Rooney, A.P.; Haigh, S.J.; Attfield, M.P.; Dryfe, R.A.W. Metal-Organic Framework Templated Electrodeposition of Functional Gold Nanostructures. *Electrochimica Acta.* **2016**, *222*, 361–369.
80. Tian, N.; Gao, Y.; Wu, J.; Luo, S.; Dai, W. Water-Resistant HKUST-1 Functionalized with Polydimethylsiloxane for Efficient Rubidium Ion Capture. *New J. Chem.* **2019**, *43*, 15539–15547.
81. Naseri, M.; Fotouhi, L.; Ehsani, A.; Dehghanpour, S. Facile Electrosynthesis of Nano Flower like Metal-Organic Framework and Its Nanocomposite with Conjugated Polymer as a Novel and Hybrid Electrode Material for Highly Capacitive Pseudocapacitors. *J. Colloid. Interface Sci.* **2016**, *484*, 314–319.
82. Abbasi, A.R.; Karimi, M.; Daasbjerg, K. Efficient Removal of Crystal Violet and Methylene Blue from Wastewater by Ultrasound Nanoparticles Cu-MOF in Comparison with Mechanosynthesis Method. *Ultrason. Sonochem.* **2017**, *37*, 182–191.
83. Jeong, H.; Lee, J. 3D-Superstructured Networks Comprising Fe-MIL-88A Metal-Organic Frameworks Under Mechanochemical Conditions. *Euro. J. Inorganic Chem.* **2019**, *2019*, 4597–4600.
84. Chen, Y.; Wu, H.; Liu, Z.; Sun, X.; Xia, Q.; Li, Z. Liquid-Assisted Mechanochemical Synthesis of Copper Based MOF-505 for the Separation of CO2 over CH4 or N2. *Ind. Eng. Chem. Res.* **2018**, *57*, 703–709.
85. Prochowicz, D.; Nawrocki, J.; Terlecki, M.; Marynowski, W.; Lewiński, J. Facile Mechanosynthesis of the Archetypal Zn-Based Metal–Organic Frameworks. *Inorg. Chem.* **2018**, *57*, 13437–13442.
86. Liu, C.-S.; Li, J.; Pang, H. Metal-Organic Framework-Based Materials as an Emerging Platform for Advanced Electrochemical Sensing. *Coordin. Chem. Rev.* **2020**, *410*, 213222.
87. Liu, W.; Yin, X.-B. Metal–Organic Frameworks for Electrochemical Applications. *TrAC Trends in Analytical Chemistry* **2016**, *75*, 86–96.
88. Zhang, X.; Chen, A.; Zhong, M.; Zhang, Z.; Zhang, X.; Zhou, Z.; Bu, X.-H. Metal–Organic Frameworks (MOFs) and MOF-Derived Materials for Energy Storage and Conversion. *Electrochemical Energy Reviews* **2019**, *2*, 29–104.
89. Jaouen, F.; Morozan, A. Metal-Organic Frameworks: Electrochemical Properties. In *Encyclopedia of Inorganic and Bioinorganic Chemistry*; John Wiley & Sons, Ltd., 2014; pp. 1–24 ISBN 978-1-119-95143-8.
90. Morozan, A.; Jaouen, F. Metal Organic Frameworks for Electrochemical Applications. *Energy Environ. Sci.* **2012**, *5*, 9269–9290.
91. Yang, J.; Zhao, F.; Zeng, B. One-Step Synthesis of a Copper-Based Metal–Organic Framework–Graphene Nanocomposite with Enhanced Electrocatalytic Activity. *RSC Advances* **2015**, *5*, 22060–22065.
92. Shams-Eldin, R.; Ali, A.A.; Hani, A.; Haikal, R.R.; Fahmy, H.M.; El Nashar, R.M.; Alkordi, M.H. Metal–Organic Framework Mediated Ni-Deposition on MWCNTs for Direct Methanol Fuel Cell Catalysis. *SN Appl. Sci.* **2023**, *5*, 166.
93. Stassen, I.; Styles, M.; Van Assche, T.; Campagnol, N.; Fransaer, J.; Denayer, J.; Tan, J.-C.; Falcaro, P.; De Vos, D.; Ameloot, R. Electrochemical Film Deposition of the Zirconium Metal–Organic Framework UiO-66 and Application in a Miniaturized Sorbent Trap. *Chem. Mater.* **2015**, *27*, 1801–1807.
94. Ye, W.; Li, Y.; Wang, J.; Li, B.; Cui, Y.; Yang, Y.; Qian, G. Electrochemical Detection of Trace Heavy Metal Ions Using a Ln-MOF Modified Glass Carbon Electrode. *J. Solid State Chem.* **2020**, *281*, 121032.
95. Wang, J. *Analytical Electochemistry: Wang/Electrochemistry 2E E-Bk*; John Wiley & Sons, Inc.: New York, USA, **2000**; ISBN 978-0-471-22823-3.

96. Cruz-Navarro, J.A.; Hernandez-Garcia, F.; Alvarez Romero, G.A. Novel Applications of Metal-Organic Frameworks (MOFs) as Redox-Active Materials for Elaboration of Carbon-Based Electrodes with Electroanalytical Uses. *Coordin. Chem. Rev.* **2020**, *412*, 213263.
97. Švancara, I.; Kalcher, K. Carbon Paste Electrodes. In *Electrochemistry of Carbon Electrodes*; John Wiley & Sons, Ltd., 2015; pp. 379–424 ISBN 978-3-527-69748-9.
98. Švancara, I.; Vytřas, K.; Kalcher, K.; Walcarius, A.; Wang, J. Carbon Paste Electrodes in Facts, Numbers, and Notes: A Review on the Occasion of the 50-Years Jubilee of Carbon Paste in Electrochemistry and Electroanalysis. *Electroanalysis* **2009**, *21*, 7–28.
99. Alipour, Z.; Hassaninejad-Darzi, S.K.; Asadollahi-Baboli, M. Construction of Pd-Ag/g-C3N4/CPE Electrochemical Nanosensor for Simultaneous Determination of Clozapine and Quetiapine Antipsychotic Drugs. *J.Alloys and Comp.* **2023**, *941*, 168958.
100. Svancara, I.; Kalcher, K.; Walcarius, A.; Vytras, K. *Electroanalysis with Carbon Paste Electrodes*; CRC Press, 2012; ISBN 978-1-4398-3019-2.
101. Fazl, F.; Gholivand, M.B. High Performance Electrochemical Method for Simultaneous Determination Dopamine, Serotonin, and Tryptophan by ZrO2–CuO Co-Doped CeO2 Modified Carbon Paste Electrode. *Talanta.* **2022**, *239*, 122982.
102. Bi, W.; Wang, G.; Hu, X. Fabrication of Zn-MOF Derived Graphitic Carbon Materials with Mesoporous Structure for Adsorptive Removal of Ceftazidime from Aqueous Solutions. *Colloid. Surf. A: Physicochem. Eng. A.* **2022**, *652*, 129758.
103. Wang, H.; Hu, Q.; Meng, Y.; Jin, Z.; Fang, Z.; Fu, Q.; Gao, W.; Xu, L.; Song, Y.; Lu, F. Efficient Detection of Hazardous Catechol and Hydroquinone with MOF-RGO Modified Carbon Paste Electrode. *J. Hazard. Mat.* **2018**, *353*, 151–157.
104. Kumari, N.; Sareen, S.; Verma, M.; Sharma, S.; Sharma, A.; Sohal, H.S.; Mehta, S.K.; Park, J.; Mutreja, V. Zirconia-Based Nanomaterials: Recent Developments in Synthesis and Applications. *Nanoscale Adv* 4, 4210–4236.
105. Chikere, Chrys.O.; Faisal, N.H.; Kong-Thoo-Lin, P.; Fernandez, C. Interaction between Amorphous Zirconia Nanoparticles and Graphite: Electrochemical Applications for Gallic Acid Sensing Using Carbon Paste Electrodes in Wine. *Nanomaterials (Basel)* **2020**, *10*, 537.
106. Petit, C.; Bandosz, T.J. Synthesis, Characterization, and Ammonia Adsorption Properties of Mesoporous Metal–Organic Framework (MIL(Fe))–Graphite Oxide Composites: Exploring the Limits of Materials Fabrication. *Adv. Funct. Mat.* **2011**, *21*, 2108–2117.
107. Wu, L.; Lu, Z.; Ye, J. Enzyme-Free Glucose Sensor Based on Layer-by-Layer Electrodeposition of Multilayer Films of Multi-Walled Carbon Nanotubes and Cu-Based Metal Framework Modified Glassy Carbon Electrode. *Biosensors and Bioelectronics.* **2019**, *135*, 45–49.
108. Sharma, S. Glassy Carbon: A Promising Material for Micro- and Nanomanufacturing. *Materials.* **2018**, *11*, 1857.
109. Arul, P.; John, S.A. Silver Nanoparticles Built-in Zinc Metal Organic Framework Modified Electrode for the Selective Non-Enzymatic Determination of H2O2. *Electrochimica Acta.* **2017**, *235*, 680–689.
110. Labib, M.; Sargent, E.H.; Kelley, S.O. Electrochemical Methods for the Analysis of Clinically Relevant Biomolecules. *Chem. Rev.* **2016**, *116*, 9001–9090.
111. Dhanjai; Sinha, A.; Lu, X.; Wu, L.; Tan, D.; Li, Y.; Chen, J.; Jain, R. Voltammetric Sensing of Biomolecules at Carbon Based Electrode Interfaces: A Review. *TrAC Trends Anal. Chem*. **2018**, *98*, 174–189.
112. Park, S.; Boo, H.; Chung, T.D. Electrochemical Non-Enzymatic Glucose Sensors. *Analytica Chimica Acta* **2006**, *556*, 46–57.
113. Sarma, A.K.; Vatsyayan, P.; Goswami, P.; Minteer, S.D. Recent Advances in Material Science for Developing Enzyme Electrodes. *Biosensors and Bioelectronics.* **2009**, *24*, 2313–2322.
114. Zhang, L.; Li, S.; Xin, J.; Ma, H.; Pang, H.; Tan, L.; Wang, X. A Non-Enzymatic Voltammetric Xanthine Sensor Based on the Use of Platinum Nanoparticles Loaded with a Metal-Organic Framework of Type MIL-101(Cr). Application to Simultaneous Detection of Dopamine, Uric Acid, Xanthine and Hypoxanthine. *Microchim Acta.* **2018**, *186*, 9.
115. Zhou, R.; Zhuang, X.; Wu, Q.; Jin, M.; Zheng, C.; Jiang, Y.; Lou, Y.; Zheng, L. Cu-MOF@Pt 3D Nanocomposites Prepared by One-Step Wrapping Method with Peroxidase-like Activity for Colorimetric Detection of Glucose. *Colloids and Surfaces B: Biointerfaces.* **2022**, *216*, 112601.

116. Yin, H.; Zhu, J.; Chen, J.; Gong, J.; Nie, Q. MOF-Derived in Situ Growth of Carbon Nanotubes Entangled Ni/NiO Porous Polyhedrons for High Performance Glucose Sensor. *Materials Letters*. **2018**, *221*, 267–270.
117. Arul, P.; JOHN, S.A. Electrodeposition of CuO from Cu-MOF on Glassy Carbon Electrode: A Non-Enzymatic Sensor for Glucose. *J. Electroanal. Chem.* **2017**, *799*.
118. Shahrokhian, S.; Khaki Sanati, E.; Hosseini, H. Direct Growth of Metal-Organic Frameworks Thin Film Arrays on Glassy Carbon Electrode Based on Rapid Conversion Step Mediated by Copper Clusters and Hydroxide Nanotubes for Fabrication of a High Performance Non-Enzymatic Glucose Sensing Platform. *Biosensors and Bioelectronics* **2018**, *112*, 100–107.
119. Wu, L.; Lu, Z.-W.; Ma, Y.; Zhang, J.-J.; Mo, G.-Q.; Du, H.-J.; Ye, J.-S. Cu(II) Metal-Organic Framework Encapsulated in Carbon Paste Electrode for High-Performance Non-Enzymatic Glucose Sensing. *Chinese J. Anal. Chem.* **2020**, *48*, e20038–e20046.
120. Zhang, L.; Li, S.; Xin, J.; Ma, H.; Pang, H.; Tan, L.; Wang, X. A Non-Enzymatic Voltammetric Xanthine Sensor Based on the Use of Platinum Nanoparticles Loaded with a Metal-Organic Framework of Type MIL-101(Cr). Application to Simultaneous Detection of Dopamine, Uric Acid, Xanthine and Hypoxanthine. *Microchim Acta.* **2018**, *186*, 9.
121. Feng, X.; Yin, X.; Bo, X.; Guo, L. An Ultrasensitive Luteolin Sensor Based on MOFs Derived CuCo Coated Nitrogen-Doped Porous Carbon Polyhedron. *Sensors and Actuators B: Chemical* **2019**, *281*, 730–738.
122. Zheng, Y.-Y.; Li, C.-X.; Ding, X.-T.; Yang, Q.; Qi, Y.-M.; Zhang, H.-M.; Qu, L.-T. Detection of Dopamine at Graphene-ZIF-8 Nanocomposite Modified Electrode. *Chinese Chemical Letters* **2017**, *28*, 1473–1478.
123. Hosseini, H.; Ahmar, H.; Dehghani, A.; Bagheri, A.; Tadjarodi, A.; Fakhari, A.R. A Novel Electrochemical Sensor Based on Metal-Organic Framework for Electro-Catalytic Oxidation of L-Cysteine. *Biosensors and Bioelectronics* **2013**, *42*, 426–429.
124. Duan, D.; Si, X.; Ding, Y.; Li, L.; Ma, G.; Zhang, L.; Jian, B. A Novel Molecularly Imprinted Electrochemical Sensor Based on Double Sensitization by MOF/CNTs and Prussian Blue for Detection of 17β-Estradiol. *Bioelectrochemistry* **2019**, *129*, 211–217.
125. He, J.; Yang, H.; Zhang, Y.; Yu, J.; Miao, L.; Song, Y.; Wang, L. Smart Nanocomposites of Cu-Hemin Metal-Organic Frameworks for Electrochemical Glucose Biosensing. *Sci Rep* **2016**, *6*, 36637.
126. Singh, R.; Musameh, M.; Gao, Y.; Ozcelik, B.; Mulet, X.; M. Doherty, C. Stable MOF@enzyme Composites for Electrochemical Biosensing Devices. *J. Mat. Chem.* **2021**, *9*, 7677–7688.
127. Hou, C.; Zhao, D.; Wang, Y.; Zhang, S.; Li, S. Preparation of Magnetic Fe3O4/PPy@ZIF-8 Nanocomposite for Glucose Oxidase Immobilization and Used as Glucose Electrochemical Biosensor. *J. Electroanal. Chem.* **2018**, *822*, 50–56.
128. Arul, P.; Gowthaman, N.S.K.; John, S.A.; Tominaga, M. Tunable Electrochemical Synthesis of 3D Nucleated Microparticles like Cu-BTC MOF-Carbon Nanotubes Composite: Enzyme Free Ultrasensitive Determination of Glucose in a Complex Biological Fluid. *Electrochimica Acta.* **2020**, *354*, 136673.
129. Li, Y.; Shen, Y.; Zhang, Y.; Zeng, T.; Wan, Q.; Lai, G.; Yang, N. A UiO-66-NH2/Carbon Nanotube Nanocomposite for Simultaneous Sensing of Dopamine and Acetaminophen. *Analytica Chimica Acta.* **2021**, *1158*, 338419.
130. Tran, T.Q.N.; Das, G.; Yoon, H.H. Nickel-Metal Organic Framework/MWCNT Composite Electrode for Non-Enzymatic Urea Detection. *Sensors and Actuators B: Chemical*. **2017**, *243*, 78–83.
131. Dang, W.; Sun, Y.; Jiao, H.; Xu, L.; Lin, M. AuNPs-NH2/Cu-MOF Modified Glassy Carbon Electrode as Enzyme-Free Electrochemical Sensor Detecting H2O2. *J. Electroanal. Chem.***2020**, *856*, 113592.
132. Yang, L.; Xu, C.; Ye, W.; Liu, W. An Electrochemical Sensor for H2O2 Based on a New Co-Metal-Organic Framework Modified Electrode. *Sensors and Actuators B: Chemical* **2015**, *215*, 489–496.
133. Lisanti, M.P.; Martinez-Outschoorn, U.E.; Lin, Z.; Pavlides, S.; Whitaker-Menezes, D.; Pestell, R.G.; Howell, A.; Sotgia, F. Hydrogen Peroxide Fuels Aging, Inflammation, Cancer Metabolism and Metastasis. *Cell Cycle.* **2011**, *10*, 2440–2449.
134. Asadian, E.; Shahrokhian, S.; Iraji Zad, A. Highly Sensitive Nonenzymetic Glucose Sensing Platform Based on MOF-Derived NiCo LDH Nanosheets/Graphene Nanoribbons Composite. *J. Electroanal. Chem.* **2018**, *808*, 114–123.
135. Sherino, B.; Mohamad, S.; Abdul Halim, S.N.; Abdul Manan, N.S. Electrochemical Detection of Hydrogen Peroxide on a New Microporous Ni–Metal Organic Framework Material-Carbon Paste Electrode. *Sensors and Actuators B: Chemical.* **2018**, *254*, 1148–1156.

136. Li, C.; Wu, R.; Zou, J.; Zhang, T.; Zhang, S.; Zhang, Z.; Hu, X.; Yan, Y.; Ling, X. MNPs@anionic MOFs/ERGO with the Size Selectivity for the Electrochemical Determination of H2O2 Released from Living Cells. *Biosensors and Bioelectronics.* **2018**, *116*, 81–88.
137. Zhao, L.; Sun, K.; Youliwasi, N.; Guo, H.; Yang, G.; Jiao, F.; Dong, B.; Chai, Y.; Mintova, S.; Liu, C. Highly Sensitive H2O2 Sensor Based on Porous Bimetallic Oxide Ce1−xTbxOy Derived from Homeotypic Ln-MOFs. *Applied Surface Science*. **2019**, *470*, 91–98.
138. Zhang, C.; Wang, M.; Liu, L.; Yang, X.; Xu, X. Electrochemical Investigation of a New Cu-MOF and Its Electrocatalytic Activity towards H2O2 Oxidation in Alkaline Solution. *Electrochemistry Communications.* **2013**, *33*, 131–134.
139. Naseri, M.; Fotouhi, L.; Ehsani, A. Nanostructured Metal Organic Framework Modified Glassy Carbon Electrode as a High Efficient Non-Enzymatic Amperometric Sensor for Electrochemical Detection of H_2O_2. *J. Electrochem. Sci. Technol*. **2018**, *9*, 28–36.
140. Meng, W.; Xu, S.; Dai, L.; Li, Y.; Zhu, J.; Wang, L. An Enhanced Sensitivity towards H2O2 Reduction Based on a Novel Cu Metal–Organic Framework and Acetylene Black Modified Electrode. *Electrochimica Acta.* **2017**, *230*, 324–332.
141. Zhang, D.; Zhang, J.; Zhang, R.; Shi, H.; Guo, Y.; Guo, X.; Li, S.; Yuan, B. 3D Porous Metal-Organic Framework as an Efficient Electrocatalyst for Nonenzymatic Sensing Application. *Talanta.* **2015**, *144*, 1176–1181.
142. Cobos, M.; De-La-Pinta, I.; Quindós, G.; Fernández, M.J.; Fernández, M.D. Graphene Oxide–Silver Nanoparticle Nanohybrids: Synthesis, Characterization, and Antimicrobial Properties. *Nanomaterials.* **2020**, *10*, 376.
143. Zhang, D.; Zhang, J.; Shi, H.; Guo, X.; Guo, Y.; Zhang, R.; Yuan, B. Redox-Active Microsized Metal-Organic Framework for Efficient Nonenzymatic H2O2 Sensing. *Sensors and Actuators B: Chemical*. **2015**, *221*, 224–229.
144. Lopa, N.S.; Rahman, Md.M.; Ahmed, F.; Chandra Sutradhar, S.; Ryu, T.; Kim, W. A Base-Stable Metal-Organic Framework for Sensitive and Non-Enzymatic Electrochemical Detection of Hydrogen Peroxide. *Electrochimica Acta.* **2018**, *274*, 49–56.
145. Wang, M.-Q.; Zhang, Y.; Bao, S.-J.; Yu, Y.-N.; Ye, C. Ni(II)-Based Metal-Organic Framework Anchored on Carbon Nanotubes for Highly Sensitive Non-Enzymatic Hydrogen Peroxide Sensing. *Electrochimica Acta.* **2016**, *190*, 365–370.
146. Liu, X.; Chen, W.; Lian, M.; Chen, X.; Lu, Y.; Yang, W. Enzyme Immobilization on ZIF-67/MWCNT Composite Engenders High Sensitivity Electrochemical Sensing. *J. Electroanal. Chem.* **2019**, *833*, 505–511.
147. Real-Time Electrochemical Quantification of H2O2 in Living Cancer Cells Using Bismuth Based MOF. *J. Electroanal. Chem.* **2022**, *914*, 116255.
148. Liu, B.; Wang, X.; Zhai, Y.; Zhang, Z.; Liu, H.; Li, L.; Wen, H. Facile Preparation of Well Conductive 2D MOF for Nonenzymatic Detection of Hydrogen Peroxide: Relationship between Electrocatalysis and Metal Center. *J. Electroanal. Chem.* **2020**, *858*, 113804.
149. Yadav, D.K.; Ganesan, V.; Sonkar, P.K.; Gupta, R.; Rastogi, P.K. Electrochemical Investigation of Gold Nanoparticles Incorporated Zinc Based Metal-Organic Framework for Selective Recognition of Nitrite and Nitrobenzene. *Electrochimica Acta.* **2016**, *200*, 276–282.
150. Ioi, J.D.; Zhou, T.; Tsao, R.; F. Marcone, M. Mitigation of Patulin in Fresh and Processed Foods and Beverages. *Toxins.* **2017**, *9*, 157.
151. Afzali, Z.; Mohadesi, A.; Ali Karimi, M.; Fathirad, F. A Highly Selective and Sensitive Electrochemical Sensor Based on Graphene Oxide and Molecularly Imprinted Polymer Magnetic Nanocomposite for Patulin Determination. *Microchemical Journal.* **2022**, *177*, 107215.
152. Shi, Y.; Zhang, Y.; Wang, Y.; Huang, H.; Ma, J. Amperometric Sensing of Paracetamol Using a Glassy Carbon Electrode Modified with a Composite of Water–Stable Metal–Organic Framework and Gold Nanoparticles. *Int. J. Electrochem. Sci.* **2018**, *13*, 7643–7654.
153. Hadi, M.; Poorgholi, H.; Mostaanzadeh, H. Determination of Metformin at Metal-Organic Framework (Cu-BTC) Nanocrystals/Multi-Walled Carbon Nanotubes Modified Glassy Carbon Electrode : Research Article. *South African Journal of Chemistry.* **2016**, *69*, 132–139.
154. Xiao, L.; Xu, R.; Yuan, Q.; Wang, F. Highly Sensitive Electrochemical Sensor for Chloramphenicol Based on MOF Derived Exfoliated Porous Carbon. *Talanta.* **2017**, *167*, 39–43.

155. Kung, C.-W.; Chang, T.-H.; Chou, L.-Y.; Hupp, J.T.; Farha, O.K.; Ho, K.-C. Porphyrin-Based Metal–Organic Framework Thin Films for Electrochemical Nitrite Detection. *Electrochemistry Communications.* **2015**, *58*, 51–56.
156. Yuan, B.; Zhang, J.; Zhang, R.; Shi, H.; Wang, N.; Li, J.; Ma, F.; Zhang, D. Cu-Based Metal–Organic Framework as a Novel Sensing Platform for the Enhanced Electro-Oxidation of Nitrite. *Sensors and Actuators B: Chemical.* **2016**, *222*, 632–637.
157. Zhang, Y.; Bo, X.; Nsabimana, A.; Han, C.; Li, M.; Guo, L. Electrocatalytically Active Cobalt-Based Metal–Organic Framework with Incorporated Macroporous Carbon Composite for Electrochemical Applications. *J. Mater. Chem. A.* **2014**, *3*, 732–738.
158. Li, J.; Xia, J.; Zhang, F.; Wang, Z.; Liu, Q. An Electrochemical Sensor Based on Copper-Based Metal-Organic Frameworks-Graphene Composites for Determination of Dihydroxybenzene Isomers in Water. *Talanta.* **2018**, *181*, 80–86.
159. Wang, Y.; Wang, L.; Chen, H.; Hu, X.; Ma, S. Fabrication of Highly Sensitive and Stable Hydroxylamine Electrochemical Sensor Based on Gold Nanoparticles and Metal–Metalloporphyrin Framework Modified Electrode. *ACS Appl. Mater. Interfaces.* **2016**, *8*, 18173–18181.
160. Zhang, J.; Xu, X.; Chen, L. An Ultrasensitive Electrochemical Bisphenol A Sensor Based on Hierarchical Ce-Metal-Organic Framework Modified with Cetyltrimethylammonium Bromide. *Sensors and Actuators B: Chemical.* **2018**, *261*, 425–433.
161. Cheng, Y.; Ma, B.; Tan, C.-P.; Lai, O.-M.; Panpipat, W.; Cheong, L.-Z.; Shen, C. Hierarchical Macro-Microporous ZIF-8 Nanostructures as Efficient Nano-Lipase Carriers for Rapid and Direct Electrochemical Detection of Nitrogenous Diphenyl Ether Pesticides. *Sensors and Actuators B: Chemical*. **2020**, *321*, 128477.
162. Zhang, J.; Xu, X.; Qiang, Y. Ultrasensitive Electrochemical Aptasensor for Ochratoxin A Detection Using AgPt Bimetallic Nanoparticles Decorated Iron-Porphyrinic Metal-Organic Framework for Signal Amplification. *Sensors and Actuators B: Chemical.* **2020**, *312*, 127964.
163. Mahmoudi, E.; Fakhri, H.; Hajian, A.; Afkhami, A.; Bagheri, H. High-Performance Electrochemical Enzyme Sensor for Organophosphate Pesticide Detection Using Modified Metal-Organic Framework Sensing Platforms. *Bioelectrochemistry.* **2019**, *130*, 107348.
164. Balali-Mood, M.; Naseri, K.; Tahergorabi, Z.; Khazdair, M.R.; Sadeghi, M. Toxic Mechanisms of Five Heavy Metals: Mercury, Lead, Chromium, Cadmium, and Arsenic. *Frontiers in Pharmacology.* **2021**, *12*.
165. Shamim, M.A.; Zia, H.; Zeeshan, M.; Khan, M.Y.; Shahid, M. Metal Organic Frameworks (MOFs) as a Cutting-Edge Tool for the Selective Detection and Rapid Removal of Heavy Metal Ions from Water: Recent Progress. *J. Environ. Chem. Eng.* **2022**, *10*, 106991.
166. Patel, P.D. (Bio)Sensors for Measurement of Analytes Implicated in Food Safety: A Review. *TrAC Trends Anal. Chem.* **2002**, *21*, 96–115.
167. Gurusamy, L.; Anandan, S.; Wu, J.J. Chapter 18 - Nanomaterials Derived from Metal-Organic Frameworks for Energy Storage Supercapacitor Application. In *Metal-Organic Frameworks for Chemical Reactions*; Khan, A., Verpoort, F., Asiri, A.M., Hoque, M.E., Bilgrami, A.L., Azam, M., Naidu, K.C.B., Eds.; Elsevier, 2021; pp. 441–470 ISBN 978-0-12-822099-3.
168. Song, D.; Jiang, X.; Li, Y.; Lu, X.; Luan, S.; Wang, Y.; Li, Y.; Gao, F. Metal–organic Frameworks-Derived MnO2/Mn3O4 Microcuboids with Hierarchically Ordered Nanosheets and Ti3C2 MXene/Au NPs Composites for Electrochemical Pesticide Detection. *J. Hazard. Mat.* **2019**, *373*, 367–376.
169. Zhou, Y.; Li, X.; Pan, Z.; Ye, B.; Xu, M. Determination of Malachite Green in Fish by a Modified MOF-Based Electrochemical Sensor. *Food Anal. Methods.* **2019**, *12*, 1246–1254.
170. Zhang, S.; Huang, W. Simultaneous Determination of Cd2+ and Pb2+ Using a Chemically Modified Electrode. *Anal Sci.* **2001**, *17*, 983–985.
171. Nguyen, M.B.; Nga, D.; Vu, T.T.; Piro, B.; PHAM TRUONG, T.N.; Yen, P.; Le, G.; Hung, L.; Vu, T.; Ha, V. Novel Nanoscale Yb-MOF Used as Highly Efficient Electrode for Simultaneous Detection of Heavy Metal Ions. *J. Materials Sci.* **2021**, *56*.
172. Roushani, M.; Valipour, A.; Saedi, Z. Electroanalytical Sensing of Cd2+ Based on Metal–Organic Framework Modified Carbon Paste Electrode. *Sensors and Actuators B: Chemical.* **2016**, *233*, 419–425.
173. Yin, H.; He, H.; Li, T.; Hu, M.; Huang, W.; Wang, Z.; Yang, X.; Yao, W.; Xiao, F.; Wu, Y.; et al. Ultra-Sensitive Detection of Multiplexed Heavy Metal Ions by MOF-Derived Carbon Film Encapsulating BiCu Alloy Nanoparticles in Potable Electrochemical Sensing System. *Analytica Chimica Acta.* **2023**, *1239*, 340730.

174. Wang, Y.; Wu, Y.; Xie, J.; Hu, X. Metal–Organic Framework Modified Carbon Paste Electrode for Lead Sensor. *Sensors and Actuators B: Chemical*. **2013**, *177*, 1161–1166.
175. Huo, D.; Zhang, Y.; Li, N.; Ma, W.; Liu, H.; Xu, G.; Li, Z.; Yang, M.; Hou, C. Three-Dimensional Graphene/Amino-Functionalized Metal–Organic Framework for Simultaneous Electrochemical Detection of Cd(II), Pb(II), Cu(II), and Hg(II). *Anal. Bioanal. Chem.* **2022**, *414*, 1575–1586.
176. Wang, F.-F.; Liu, C.; Yang, J.; Xu, H.-L.; Pei, W.-Y.; Ma, J.-F. A Sulfur-Containing Capsule-Based Metal-Organic Electrochemical Sensor for Super-Sensitive Capture and Detection of Multiple Heavy-Metal Ions. *Chem. Eng. J.* **2022**, *438*.
177. Ru, J.; Wang, X.; Cui, X.; Wang, F.; Ji, H.; Du, X.; Lu, X. GaOOH-Modified Metal-Organic Frameworks UiO-66-NH2: Selective and Sensitive Sensing Four Heavy-Metal Ions in Real Wastewater by Electrochemical Method. *Talanta.* **2021**, *234*, 122679.
178. Wang, Y.; Ge, H.; Wu, Y.; Ye, G.; Chen, H.; Hu, X. Construction of an Electrochemical Sensor Based on Amino-Functionalized Metal-Organic Frameworks for Differential Pulse Anodic Stripping Voltammetric Determination of Lead. *Talanta* **2014**, *129*, 100–105.
179. Chen, X.; Zhao, J.-X.; Wang, J.-W.; Liu, Y.; Wang, L.-C.; Weerasooriya, R.; Wu, Y.-C. Doping ZIF-67 with Transition Metals Results in Bimetallic Centers for Electrochemical Detection of Hg(II). *Electrochimica Acta.* **2021**, *387*, 138539.
180. Niu, B.; Yao, B.; Zhu, M.; Guo, H.; Ying, S.; Chen, Z. Carbon Paste Electrode Modified with Fern Leave-like MIL-47(as) for Electrochemical Simultaneous Detection of Pb(II), Cu(II) and Hg(II). *J. Electroanal. Chem.* **2021**, *886*, 115121.
181. Quang Khieu, D.; Thi Thanh, M.; Vinh Thien, T.; Hai Phong, N.; Hoang Van, D.; Dinh Du, P.; Phi Hung, N. Synthesis and Voltammetric Determination of Pb(II) Using a ZIF-8-Based Electrode. *J. Chem.***2018**, *2018*.
182. Lu, M.; Deng, Y.; Luo, Y.; Lv, J.; Li, T.; Xu, J.; Chen, S.-W.; Wang, J. Graphene Aerogel–Metal–Organic Framework-Based Electrochemical Method for Simultaneous Detection of Multiple Heavy-Metal Ions. *Anal. Chem.* **2019**, *91*, 888–895.
183. D. Pournara, A.; Margariti, A.; D. Tarlas, G.; Kourtelaris, A.; Petkov, V.; Kokkinos, C.; Economou, A.; S. Papaefstathiou, G.; J. Manos, M. A Ca 2+ MOF Combining Highly Efficient Sorption and Capability for Voltammetric Determination of Heavy Metal Ions in Aqueous Media. *J. Materials Chem. A*. **2019**, *7*, 15432–15443.
184. Ma, L.; Zhang, X.; Ikram, M.; Ullah, M.; Wu, H.; Shi, K. Controllable Synthesis of an Intercalated ZIF-67/EG Structure for the Detection of Ultratrace Cd2+, Cu2+, Hg2+ and Pb2+ Ions. *Chem. Eng. J.* **2020**, *395*, 125216.
Yang, H.; Peng, C.; Han, J.; Song, Y.; Wang, L. Three-Dimensional Macroporous Carbon/Zr-2,5-Dimercaptoterephthalic Acid Metal-Organic Frameworks Nanocomposites for Removal and Detection of Hg(II). *Sensors and Actuators B: Chemical.* **2020**, *320*, 12844.